Brain-Controlled Epidural Stimulation Reveals Enhanced Corticospinal Excitability and Upper-Limb Function in Chronic Tetraplegia

Atsushi Sasaki[1,2,3,†], Rizaldi Ahmad Fadli[1,4,†], Akiko Yuasa[1,2,5,6], Zachary Boogaart[1,4,7], Hiroki Saito[8,9], Nevena Musikic[1], Roberto de Freitas[10,11], Nicolo Macellari[10,11], Kevin C. Davis[1,4,7], Nilanjana Datta[1], Guilherme S. Piedade[2], Seth Tigchelaar[2], Michael E. Ivan[2], W. Dalton Dietrich[1,2,4], Naaz Desai[12], Vera Zivanovic[12], Milos R. Popovic[12,13,14], Elvira Pirondini[10,11,15], Jonathan Jagid[2], Abhishek Prasad[1,2,4], James D. Guest[1,2], Marco Capogrosso[10,11,15], Joacir Graciolli Cordeiro[2], Matija Milosevic[1,2,4,*]

[1]The Miami Project to Cure Paralysis, University of Miami Miller School of Medicine, FL, USA.
[2]Department of Neurological Surgery, University of Miami Miller School of Medicine, FL, USA.
[3]Graduate School of Arts and Sciences, The University of Tokyo, Tokyo, Japan.
[4]Department of Biomedical Engineering, University of Miami, FL, USA.
[5]Faculty of Medicine, Fujita Health University, Aichi, Japan.
[6]Japan Society for the Promotion of Science, Tokyo, Japan.
[7]Medical Scientist Training Program, University of Miami Miller School of Medicine, FL, USA.
[8]Department of Rehabilitation, Tokyo University of Technology, Tokyo, Japan.
[9]Center for Human Movement, Tokyo University of Technology, Tokyo, Japan.
[10]Rehab Neural Engineering Labs, University of Pittsburgh, Pittsburgh, PA, USA.
[11]Department of Neurological Surgery, University of Pittsburgh, Pittsburgh, PA, USA.
[12]KITE Research Institute – University Health Network, Toronto, ON, Canada.
[13]Institute of Biomedical Engineering, University of Toronto, Toronto, ON, Canada.
[14]CRANIA, University Health Network, Toronto, ON, Canada.
[15]Department of Bioengineering, University of Pittsburgh, Pittsburgh, PA, USA.

[†]These two authors contributed equally to this work and are designated as co-first authors

***Corresponding author**:
Matija Milosevic, PhD
The Miami Project to Cure Paralysis
University of Miami Miller School of Medicine
1095 NW 14th Terrace
Miami, FL 33136, USA
Phone: 305-243-3572
Fax: 305-243-3913
E-mail: mmilosevic@med.miami.edu

Number of pages: 42
Number of figures: 8
Number of extended data figures and tables: 3 figures and 2 tables
Number of supplementary figures and tables: 8 figures and 10 tables

Abstract (175 words)
Spinal cord injury disrupts corticospinal transmission and impairs voluntary motor control. While epidural spinal cord stimulation (ESCS) can augment residual motor output, its capacity to drive long-term neuroplasticity remains unoptimized. Here, we present a first-in-human case study showing that an implantable brain-computer interface (BCI) paired with cervical ESCS can potentiate corticospinal connectivity, leading to immediate and sustained improvements in upper-limb motor function in an individual with chronic, motor-complete cervical SCI. The BCI decoded motor intent from electrocorticography signals to trigger stimulation at intent onset, coupling ESCS to volitional movement attempts. This BCI-ESCS paradigm enhanced grip strength and object manipulation immediately and produced greater increases in corticospinal excitability after a single session compared to tonic ESCS. Notably, a four-week BCI-ESCS therapy led to clinically meaningful improvements in voluntary hand function even without system assistance, with some gains persisting one-month post-therapy. These proof-of-concept findings suggest that intention-driven neuromodulation may induce corticospinal plasticity, offering a mechanistically driven neuromotor recovery approach. Overall, BCI-ESCS reveals enhanced volitional control even in an individual with severe paralysis deemed at the recovery plateau.

Keywords: spinal cord injury, brain-computer interface, cervical epidural spinal cord stimulation, corticospinal plasticity, neurorehabilitation, tetraplegia, electrocorticography.

1. Introduction

Spinal cord injury (SCI) is a life-altering condition that disrupts motor and sensory pathways, leading to severe impairments in voluntary motor control. Among individuals with cervical SCI, tetraplegia significantly limits upper limb function, reducing independence and quality of life[1]. Approximately two-thirds of SCIs occur at the cervical level (63.4% at C1–C7), often resulting in tetraplegia and impairing upper limb control[2]. While individuals with incomplete injuries (American Spinal Injury Association Impairment Scale (AIS) B-D) retain some degree of sensorimotor function, those with complete injuries (AIS A) typically exhibit low to no voluntary movement below the lesion level with minimal recovery potential[3,4]. Despite extensive rehabilitation efforts, standard physical and occupational therapy often leads to limited motor recovery, necessitating novel neuromodulatory strategies to optimize residual connections and promote upper limb function restoration.

Epidural spinal cord stimulation (ESCS) has emerged as a promising tool for restoring motor function by reactivating spinal networks below the lesion. Early studies demonstrated that ESCS can facilitate volitional lower-limb movement in individuals with chronic paraplegia[5–9]. The potential of ESCS to restore upper limb function was later explored in non-human primates, where cervical ESCS was found to enhance voluntary reaching and grasping by modulating spinal motoneurons[10,11]. Lu et al.[12] provided human evidence that cervical ESCS can enhance voluntary hand function in individuals with chronic tetraplegia by engaging spinal circuits. More recently, Powell et al.[13] demonstrated that continuous cervical ESCS improves grip strength and movement kinematics in individuals with post-stroke hemiparesis. While these studies highlight the immediate assistive benefits of cervical ESCS, their ability to drive lasting corticospinal plasticity to support durable upper-limb recovery remains to be fully established.

Brain-computer interface (BCI) technology is another promising approach to restore volitional control in individuals with motor paralysis by decoding motor intent and providing real-time stimulation to enable upper limb muscle activation[14–16]. Unlike conventional tonic ESCS that applies stimulation continuously, BCI-controlled neuromodulation has the potential to precisely deliver stimulation based on the user's motor intent, reinforcing the link between cortical activity and spinal circuits[17,18]. Preclinical studies demonstrated that BCI-controlled neuromodulation can induce adaptive cortical changes to facilitate motor recovery in animal models[11,19,20]. Recent work by Lorach et al.[18] demonstrated that an implantable brain-spine interface can restore lower-limb function in an individual with incomplete SCI, establishing clinical feasibility for chronic intention-driven neuromodulation. However, the clinical translation of an implantable brain-spine interface for upper limb function, particularly in individuals with complete cervical SCI, has not yet been realized. Here, we present a first-in-human study investigating the effects of implantable electrocorticography (ECoG)-based BCI-ESCS therapy with a focus on corticospinal connectivity and upper-limb motor recovery in an individual with chronic complete cervical SCI (AIS A). We hypothesized that BCI-ESCS therapy would facilitate corticospinal plasticity, leading to meaningful improvements in upper limb function despite a clinically complete paralysis diagnosis.

To evaluate the therapeutic potential of an implantable BCI-ESCS strategy, we investigated the neuromodulation effects on corticospinal excitability and upper limb motor function in an individual with chronic complete tetraplegia, with primary objectives to:

1) Assess the **assistive (immediate) effects** of BCI-ESCS and Tonic-ESCS on grip strength, reaching kinematics, and hand function tests.

2) Evaluate the **single-session effects** of BCI-ESCS and Tonic-ESCS therapy on corticospinal excitability through motor evoked potentials (MEPs), spinal excitability through posterior root muscle (PRM) reflexes, and hand dexterity through functional performance tests.
3) Determine the **longitudinal (therapeutic) effects** of a four-week BCI-ESCS intervention on corticospinal connectivity, reaching performance, and clinical hand function scores.

By integrating an ECoG-based BCI with epidural spinal stimulation, this study establishes a novel implantable BCI neuromodulation approach to restore corticospinal connectivity and upper-limb motor function in chronic complete SCI. The first-in-human application of BCI-ESCS aims to advance neural restoration by engaging targeted plasticity mechanisms to re-enable volitional control of the upper limb.

2. Results

2.1. Study design and experimental setup

This study is the first to report the effects of BCI-ESCS intervention on neural excitability and upper-limb motor function recovery in an individual with complete spinal cord injury (Fig.1). The participant was a male in his 20's with a chronic (11 years post-injury) motor-complete AIS A injury at the C4–C5 level, confirmed by an ISNCSCI examination performed immediately prior to study initiation. Neurophysiological assessments supported this classification. MRI (Fig. 1) showed a focal lesion at the C4 level, and no measurable MEPs or voluntary electromyographic (EMG) activity were detected at baseline in intrinsic hand muscles (FDI, ADM, and APB) (Supplementary Fig. 1), which are innervated below the C5 level[21]. The participant had undergone anterior cervical discectomy and fusion (C3–C5) in 2015 and later received an ECoG implant over the right-hand knob area of the motor cortex in 2018 as part of another clinical trial (NCT02564419)[22,23]. In the current study, the BCI-ESCS therapy was delivered by detecting motor imagery from ECoG signals to trigger dorsal root spinal stimulation in real time during activity-based training. Motor imagery was detected using a one degree-of-freedom classifier[24–28] based on event-related desynchronization (ERD) activity from calibrated ECoG channels (Ch 0-3) within the 8-14 Hz band (Section 4.5), derived from 60 calibration trials. During therapy, the BCI detected motor imagery when the ECoG signal power remained below a predefined threshold for one second within a 15-second window after the Go cue, which triggered ESCS. The decoding success rate was 83.8±4.2 %. ESCS was delivered via two percutaneous eight-contact leads implanted in the dorsal epidural space from vertebral levels C5–T1 caudal to the injury site to enable upper limb spinal circuit neuromodulation (Fig.1). The leads were positioned unilaterally on the right side over the dorsal roots to selectively activate right upper limb motor pools[13]. Stimulation parameters were individually optimized based on spinal mapping and functional responses (Section 4.4; Extended Data Fig. 1; Supplementary Fig. 2) to facilitate volitional control while avoiding overt passive movement at rest[6,13]. On select days, additional assessments were performed with Tonic-ESCS, a control condition in which continuous stimulation was applied throughout the duration of the session. These additional sessions also enabled comparison of assistive and short-term effects between stimulation modes.

BCI-ESCS therapeutic effects were assessed through three distinct analyses: 1) Assistive effects - Immediate functional benefits of BCI-ESCS compared to no stimulation and Tonic-ESCS condition; 2) Single-session effects - Changes in neurophysiological outcomes and upper-limb motor function after a single session of BCI-ESCS compared to Tonic-ESCS intervention; and 3) Longitudinal effects - Functional and neurophysiological changes following four weeks (28 days) of BCI-ESCS therapy.

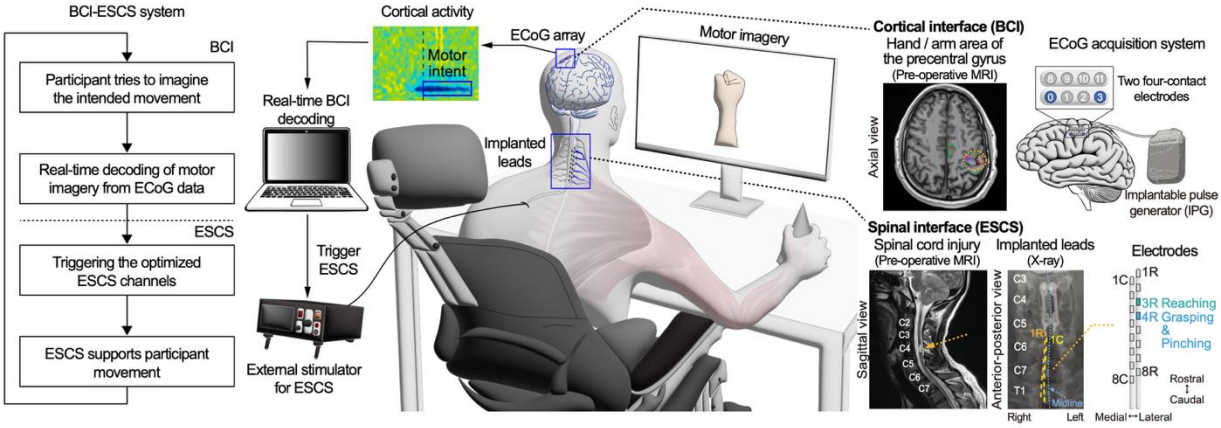

Fig. 1: Implantable BCI-ESCS system for upper limb motor rehabilitation in chronic SCI | The brain-computer interface (BCI)- epidural spinal cord stimulation (ESCS) system integrates real-time decoding of motor intent with targeted spinal cord stimulation to restore upper limb function in an individual with chronic complete cervical spinal cord injury (C4–C5; AIS A). The participant attempts to imagine the intended movement, which is detected through an implanted electrocorticography (ECoG) array placed over the precentral gyrus, as identified in preoperative MRI (from Cajigas et al.[22] with permission of Oxford University Press). ECoG signals were acquired using an implantable pulse generator (IPG), which was also used to deliver single-pulse motor cortex stimulation for motor evoked potential (MEP) measurements (Section 4.10), and ESCS was applied through an external stimulator via percutaneously implanted leads (Section 4.4). The BCI system decodes cortical activity in real time and, upon detection of motor intent, triggers an external stimulator to deliver optimized ESCS via percutaneously implanted epidural leads. The spinal X-ray image confirms the placement of epidural electrodes over the C5–T1 spinal segments, with specific channels targeting functional tasks such as reaching (e.g., 3R) and grasping/pinching (e.g., 4R). This system is designed to enhance the corticospinal network by aligning cortical activity with spinal stimulation, promoting task-specific neuromodulation and functional recovery.

2.2. Assistive effects - Grip strength, reaching function, and hand motor function improve during BCI-ESCS and Tonic-ESCS

To assess the assistive effects of BCI-ESCS and Tonic-ESCS, we compared three conditions: no stimulation (no-stim), Tonic-ESCS (continuous stimulation), and BCI-ESCS (stimulation triggered by motor intent). For these assistive-effect comparisons, ESCS stimulation parameters, including the contact, amplitude, and frequency, were matched between Tonic-ESCS and BCI-ESCS (Fig. 2). During the first week post-implant, maximum grip force and EMG activity were measured during gripping tasks for 5 seconds in different conditions. Both stimulation modalities increased grip force compared to no stimulation (no-stim: 0.5±0.2 N; Tonic-ESCS: 9.9±1.0 N; BCI-ESCS: 20.3±10.0 N) (Fig. 2a and Supplementary Table 1). Similarly, EMG recordings from the flexor carpi radialis (FCR) and extensor carpi radialis (ECR) muscles revealed minimal activity in the no stimulation condition, whereas both Tonic- and BCI-ESCS increased volitional EMG activation (FCR, no-stim: 0.008±0.001 mV; Tonic-ESCS: 0.065±0.001 mV; BCI-ESCS: 0.108±0.006 mV; ECR, no-stim: 0.012±0.001 mV; Tonic-ESCS: 0.031±0.004 mV; BCI-ESCS: 0.075±0.015 mV). Notably, BCI-ESCS elicited the highest grip force and EMG activity, indicating a greater enhancement of volitional motor output compared to Tonic-ESCS (Fig. 2a).

Upper limb coordination during the second week after implantation was evaluated using a three-dimensional (3D) reaching task toward four positions (left, right, center, and upward) under each stimulation condition (Fig. 2b). Movement smoothness improved for most targets under both Tonic-ESCS and BCI-ESCS compared to no stimulation, as reflected by reduced numbers of

velocity peaks[13], and differences between stimulation modes were not observed for most targets (Fig. 2c). Endpoint accuracy was quantified as target error, defined as the 3D distance between the final wrist position and the target at reach termination[29]. Target error was generally reduced (i.e., accuracy improved) under both stimulation conditions compared with no stimulation (Fig. 2c), with reductions tending to be larger under BCI-ESCS. Consistently, path length and reaching time increased under BCI-ESCS (Supplementary Fig. 3). Analysis of the initial direction angle, which quantifies deviation from the optimal straight-line trajectory[29,30], revealed that BCI-ESCS produced larger deviations than the other conditions, suggesting more abrupt movement initiation caused by intent-triggered stimulation (Fig. 2c).

We also conducted muscle synergy analysis using EMG data recorded from 16 muscles spanning the shoulder, upper arm, and forearm during reaching movements to investigate upper limb coordination (Supplementary Information 1.1). Six synergies were identified under no stimulation, whereas seven synergies were identified under both Tonic-ESCS and BCI-ESCS (Extended Data Fig. 2), indicating that both stimulation conditions shifted the synergy structure from broad co-activation patterns toward sparser and more functionally distinct muscle groupings[31,32]. Additionally, only the BCI-ESCS condition exhibited a more evident contribution of scapular stabilizers (i.e., lower trapezius-dominant synergy), whereas Tonic-ESCS retained a biceps-dominant synergy similar to the no-stimulation condition. Details on synergy patterns and their functional implications are provided in Supplementary Information 1.2.

Consistent with improvements in grip strength and reaching function, the Toronto Rehabilitation Institute-Hand Function Test (TRI-HFT) scores also showed immediate improvement under both BCI-ESCS and Tonic-ESCS (Fig. 2d). Notably, in the mobile phone task, the no stimulation condition yielded a score of 2 points, whereas both BCI-ESCS and Tonic-ESCS improved the score to 4 points. Similarly, in the rectangular blocks task, improvements of 2–3 points were recorded with both BCI-ESCS and Tonic-ESCS across most weights and surface friction levels, except the 100 g high friction task, where no differences were observed. These improvements in clinical scores likely stem from improved grip strength and reaching function during ESCS, suggesting that both BCI-ESCS and Tonic-ESCS contribute to improved upper limb motor performance. However, no differences were observed between BCI-ESCS and Tonic-ESCS conditions immediately during the stimulation.

Overall, these findings demonstrate that both BCI-ESCS and Tonic-ESCS can immediately enhance the motor function of an individual with complete SCI, with BCI-ESCS potentially providing additional benefits particularly in grip force magnitude (Fig. 2a) as well as reaching accuracy and movement initiation (Fig. 2c).

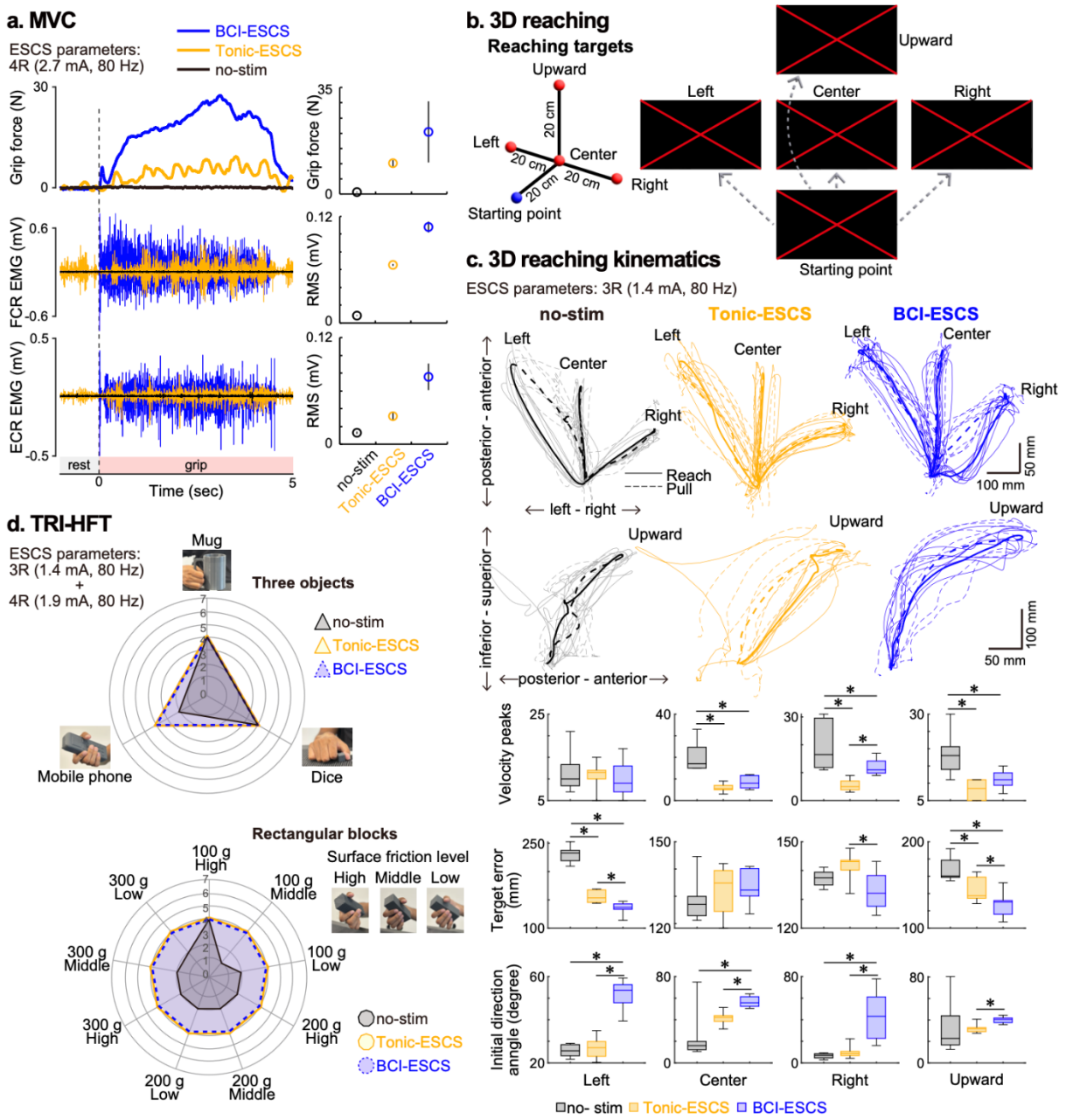

*Some images removed by authors to comply with MedRxiv publication policies

Fig. 2: BCI-ESCS and Tonic-ESCS immediately improve motor function | a. Grip strength and electromyographic (EMG) activity during maximal voluntary contraction (MVC). Representative traces of grip force and EMG activity recorded from the flexor carpi radialis (FCR) and extensor carpi radialis (ECR) muscles under no-stimulation (no-stim, black), Tonic-ESCS (yellow), and BCI-ESCS (blue) conditions. The right panel shows plots of peak grip force and root-mean-square (RMS) EMG amplitude, calculated after applying a notch filter at the stimulation frequency to attenuate potential stimulation-related components[13]. MVC was assessed with two trials per condition. **b**. 3D reaching task setup. The participant performed reaching movements towards four target positions (left, center, right, and upward) from a fixed starting position, with eight repetitions per target. **c.** Kinematic analysis of 3D reaching movements. Trajectories of reaching movements under no stim (black), Tonic-ESCS (yellow), and BCI-ESCS (blue) are shown for each target direction. Bottom panels depict boxplots of velocity peaks (movement smoothness), target error (endpoint accuracy), and initial direction angle

(deviation from the optimal straight-line trajectory), showing improved movement smoothness and endpoint accuracy under both Tonic-ESCS and BCI-ESCS compared with no stimulation, and larger initial direction angles under BCI-ESCS than the other conditions. In each boxplot, the central line indicates the median, the box represents the interquartile range (25th to 75th percentile), and the whiskers extend to the full range of the data (minimum to maximum). Statistical inference was performed using a bootstrap method (n=10,000 resamples) for datasets with n=8 observations per condition. Asterisks indicate statistical significance and rejection of the null hypothesis of no difference with a 95% CI. **d.** Functional hand assessment using the Toronto Rehabilitation Institute Hand Function Test (TRI-HFT). Radar plots show performance across object manipulation and rectangular block tasks. Both stimulation conditions improved function relative to no stimulation. Within all assistive-effect assessments, BCI-ESCS and Tonic-ESCS used identical ESCS settings (contacts, stimulation amplitude, and frequency).

2.3. Single-session BCI-ESCS, but not Tonic-ESCS, potentiates corticospinal connections

We examined the short-term neurophysiological and functional effects of a single-session BCI-ESCS and Tonic-ESCS therapy, assessed across two sessions per condition using an interleaved crossover design. The participant performed activity-based training with either BCI-ESCS or Tonic-ESCS for 28 minutes on separate days. Neurophysiological and motor performance assessments were conducted before and immediately after each session when stimulation was turned off (Fig. 3a). Corticospinal and spinal excitability were assessed as indicators of neurophysiological changes, while functional motor performance was evaluated using the nine-hole peg test (9HPT) and box and block test (BBT). The therapy, which focused on reaching, grasping, and pinching movements, was conducted with the guidance of a physical therapist. The training protocol was identical across conditions, ensuring consistency in task execution. Details of the therapy protocol are provided in the Methods section (see Section 4.6).

Corticospinal excitability was assessed by measuring MEPs from the ECR and FCR muscles, elicited via subdural ECoG electrode single-pulse motor cortex stimulation (MCS). Electrical pulses (450 µs, bipolar configuration) were delivered across a range of 4.0 to 10.5 V through the implanted pulse generator to obtain the MEP recruitment curve, and analyzed using pooled data from two sessions. Tonic-ESCS therapy showed no significant pre-post MEP changes in either muscle (Fig. 3b; Supplementary Table 2). In contrast, BCI-ESCS therapy led to a significant potentiation of MEP amplitudes compared to pre-intervention levels in both the ECR and FCR muscles. This facilitation was supported by the pooled comparison across intensities and was also observed at selected stimulation intensities (Fig. 3b, Supplementary Table 2). Together, these results are consistent with greater corticospinal facilitation following BCI-ESCS than Tonic-ESCS.

Spinal excitability was assessed through PRM reflexes, elicited by paired-pulse ESCS. Reflex responses were recorded at increasing stimulation intensities, with three paired-pulse stimuli per level, and analyzed using pooled data from two sessions. PRM recruitment was quantified relative to motor threshold (MT) defined at Pre of each session (first response >0.05 mV peak-to-peak in both ECR and FCR), and responses were analyzed from MT-0.4 mA to MT+0.6 mA. BCI-ESCS produced significant pre–post increases in PRM reflex amplitude in both ECR and FCR, whereas Tonic-ESCS produced no significant changes (Fig. 3c; Supplementary Table 3). These findings align with the MEP results, further supporting the notion that BCI-ESCS therapy enhances both corticospinal and spinal excitability, whereas Tonic-ESCS alone elicits minimal effects on these pathways.

Despite differences in neurophysiological responses, short-term motor performance improvements did not significantly differ between BCI-ESCS and Tonic-ESCS conditions. Performance on the 9HPT remained unchanged in both conditions. In the BBT, the number of

blocks increased from 4.0±0.0 to 6.0±0.0 following Tonic-ESCS therapy and from 3.0±1.4 to 3.5±0.7 following BCI-ESCS therapy.

Overall, these results indicate that a single session of BCI-ESCS, but not Tonic-ESCS, induces immediate potentiation in both corticospinal and spinal excitability, suggesting that volitionally coupled stimulation more effectively engages facilitation mechanisms. Even in the absence of immediate short-term performance differences, these findings point to advantages of BCI control to restore corticospinal integrity.

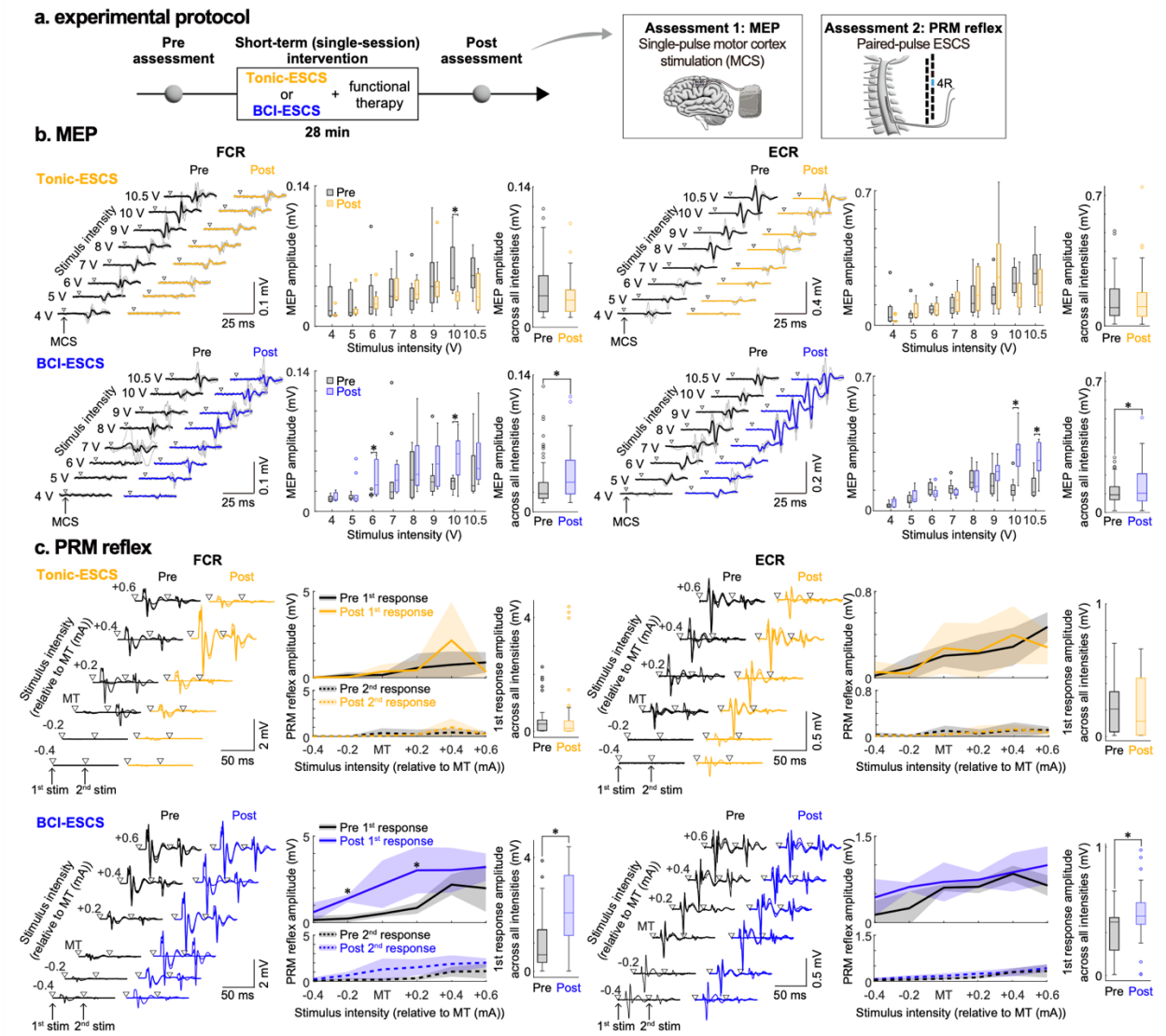

Fig. 3: Single-session BCI-ESCS therapy potentiates corticospinal connections | a. Experimental protocol. Single-session effects were assessed in an interleaved crossover design with two sessions per condition. The participant completed functional therapy sessions with either Tonic-ESCS or BCI-ESCS, with neurophysiological and motor assessments conducted before (Pre) and after (Post) intervention during stimulation-off testing. Task-specific ESCS parameters for each session are detailed in Supplementary Fig. 2. **b.** Corticospinal excitability measured via motor evoked potentials (MEPs). Left: Representative MEP waveforms from the flexor carpi radialis (FCR) and extensor carpi radialis (ECR) muscles are shown for Tonic-ESCS (yellow) and BCI-ESCS (blue). Middle: Boxplots summarize MEP amplitudes at each stimulus intensity; data were pooled across two sessions (10 trials per condition per intensity; 5 trials/session × 2 sessions). Right:

Boxplots show amplitudes pooled across all tested intensities (across-intensity summary), showing increased corticospinal excitability following BCI-ESCS but no potentiation following Tonic-ESCS. **c.** Spinal excitability assessed via posterior root muscle (PRM) reflexes elicited by paired-pulse ESCS using 4R contact. Left: Representative PRM reflex waveforms are shown for the FCR and ECR muscles. Middle: Recruitment curves (mean ± SD) summarize PRM reflexes using data pooled across two sessions (6 trials per condition per intensity; 3 paired pulses/session × 2 sessions). Right: Boxplots show PRM reflexes pooled across all intensities (across-intensity summary). Because absolute stimulation intensities differed between sessions, intensity is plotted relative to motor threshold (MT), defined at Pre of each session as the lowest intensity at which the first response exceeded 0.05 mV in both muscles. Responses were analyzed from MT-0.4 mA to MT+0.6 mA. MT values for the first session were BCI: 3.0 mA and Tonic: 2.4 mA; for the second session, BCI: 2.4 mA and Tonic: 2.2 mA. In all boxplots, the central line indicates the median, the box represents the interquartile range (25th to 75th percentile), and the whiskers extend to the full range of data. Outliers are plotted individually as circles. Statistical inference was performed using a bootstrap method (n=10,000 resamples) on the pooled datasets. Asterisks indicate statistical significance and rejection of the null hypothesis of no difference with a 95% CI.

2.4. Longitudinal effects - BCI-ESCS therapy enhances corticospinal excitability and voluntary motor function

Longitudinal therapeutic effects were investigated by evaluating the effects of a 28-day intervention using BCI-ESCS on the central nervous system excitability, voluntary motor performance, and clinical outcomes after the therapy period. Assessments were conducted at three time points: at baseline prior to ESCS implantation (Pre); post-intervention following the completion of BCI-ESCS therapy (Post); and at follow-up, one month after ESCS lead explantation (Follow-up) (Fig. 4a). BCI-ESCS therapy regimen consisted of 19 sessions over 28 days, with each therapy session lasting approximately 40 minutes (40.8±19.3 min). Three of those sessions consisted of Tonic-ESCS to evaluate assistive and short-term effects separately, allowing us to compare corticospinal excitability and short-term motor function outcomes to BCI-ESCS. The longitudinal intervention was focused on evaluating BCI-ESCS therapeutic efficacy on voluntary function following the completion of the therapy.

During the therapy, the participant performed BCI-triggered ESCS to activate the right-hand during motor tasks, including reaching, grasping, pronation, supination, and pinching. ESCS was activated in real-time upon BCI detection of motor intent, with assistance provided by the therapist as needed. Training progressed from basic movements to complex functional tasks, incorporating objects of varying size, weight, and texture to enhance motor engagement. As performance improved, tasks mimicking daily activities, such as drinking and eating, were introduced to facilitate functional recovery (see Methods section 4.6 for details regarding task progression).

Corticospinal excitability, assessed using MEPs elicited by single-pulse MCS, significantly increased following long-term BCI-ESCS therapy in both the ECR and FCR muscles (Fig. 4b; Supplementary Fig. 4; Supplementary Table 4). However, this potentiation returned to baseline levels at Follow-up, suggesting that therapy facilitates corticospinal excitability, but the effects were not retained in Follow-up after completion of the therapy in an individual with motor complete SCI.

To further evaluate upper limb coordination, we analyzed 3D reaching task performance. After therapy, velocity peaks at the center, right, and upward targets significantly decreased, suggesting smoother movements even without stimulation (Fig. 4c; Supplementary Table 5). However, at Follow-up, velocity peaks for the right and upward targets returned to pre-therapy levels. Deviation from the target (target error) also improved for most targets and tended to remain lower than Pre at Follow-up, indicating partial retention of enhanced endpoint accuracy. Consistently, increased path length and partially prolonged reaching time reflect changes in

movement execution (Supplementary Fig. 5). The initial direction angle, particularly for the Left and Right targets, also increased and remained elevated at Follow-up. Taken together, persistent improvements in endpoint accuracy and initial trajectory control, despite partial return toward baseline, suggest motor adaptation induced by BCI-ESCS therapy, which may contribute to longer-term functional improvements.

To assess neuromuscular coordination, we analyzed muscle synergy patterns during reaching movements. Before therapy, six synergies were identified, whereas seven synergies were detected post-therapy (Extended Data Fig. 3), indicating increased neuromuscular coordination complexity. However, at Follow-up, the number of synergies returned to six, mirroring trends observed in reaching performance and MEP changes. These findings suggest that long-term BCI-ESCS therapy induces transient neuromuscular adaptations, which regress after therapy cessation. Additional details on synergy analysis are provided in Supplementary Information 1.3.

Finally, we evaluated clinical scores using the TRI-HFT and Graded Redefined Assessment of Strength, Sensibility, and Prehension (GRASSP). A summary of all TRI-HFT and GRASSP scores is provided in Extended Data Tables 1-2, with overall improvements more pronounced in the therapy-targeted right hand. These findings indicate that upper limb function significantly improved after therapy and was maintained one month after the intervention.

For the right hand, the therapy target, the TRI-HFT 10 object score increased from Pre (19 points) to Post (28 points), with retained gains at Follow-up (30 points), showing notable improvements in pop can, mobile phone, paper, and credit card tasks (Fig. 4d). Notably, in the mobile phone task, the score increased from 2 points at Pre to 6 points at Post, with retained improvement at Follow-up. Similarly, in the credit card task, the score increased from 1 point at Pre to 4 points at Post and Follow-up. These gains reflect meaningful improvements in proximal arm control (shoulder and elbow), wrist coordination and forearm rotation, and grasp and pinch capability (enhanced thumb engagement), thereby supporting functional object handling. The TRI-HFT rectangular blocks task score also improved from Pre (19 points) to Post (36 points) and remained at Follow-up (36 points) (Fig. 4d).

We compared these results with a control dataset of six individuals with chronic SCI who underwent 40 sessions of conventional activity-based therapy over 16 weeks (see Methods 4.8). In the control cohort, mean gains in the right (dominant) hand were 3.3±4.9 points in the 10-object and 5.2±10.0 points in the rectangular blocks task. Following 19 sessions of BCI-ESCS therapy, our participant's right hand improved by 9 points in the 10-object task and 17 points in the rectangular blocks task, exceeding the average gains observed in the control cohort (Fig. 4d; Supplementary Table 6), and suggesting potential functional benefits. Moreover, considering combined scores across both hands (13 points in the 10-object task and 23 points in the rectangular blocks task; Extended Data Table 1), our participant demonstrated TRI-HFT improvements that exceeded the minimal detectable change (MDC) of 9.1 points in 10-objects and 9.2 points in the rectangular blocks task[33]. These gains were predominantly driven by improvements in the therapy-targeted right hand, with the untrained left hand showing minimal changes (4 points in the 10-object task and 6 points in the rectangular blocks task; Extended Data Table 1).

Similarly, GRASSP Quantitative Prehension scores revealed notable improvements only in the water bottle, jam jar, and coin tasks (Fig. 4e). The 4-point gain at Post in GRASSP-Quantitative prehension surpassed the MDC of 3 points for SCI individuals[34], which was largely maintained at Follow-up. The ISNCSCI examination also showed neurological-level changes, with a 2-point increase in total motor score, and an expansion of the zone of partial preservation by one sensory level and two motor levels (Supplementary Table 7).

Notably, the BCI-ESCS therapy did not adversely affect the participant's neurological classification (ISNCSCI, Supplementary Table 7), independence (SCIM, Supplementary Table 8), quality of life (QoL-BDS, Supplementary Table 9), or pain levels (ISCIPBDS, Supplementary Table 10), supporting the safety of the intervention.

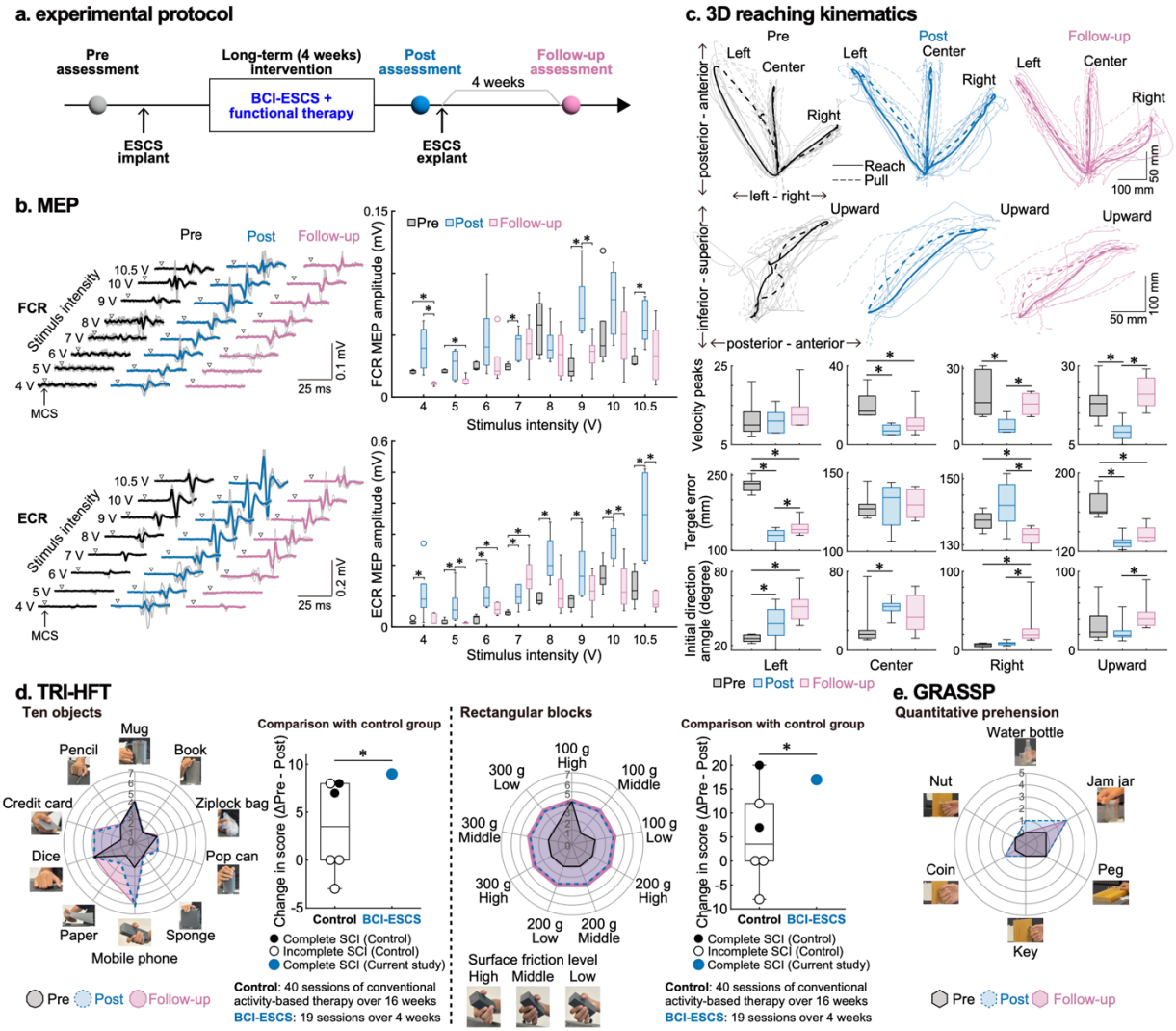

Fig. 4: Long-term BCI-ESCS therapy enhances corticospinal excitability and upper-limb motor performance | a. Experimental protocol. Assessments were conducted at Pre (baseline, before ESCS implantation), Post (after 4 weeks of BCI-ESCS therapy), and Follow-up (4 weeks after ESCS explantation) to evaluate the longitudinal effects of BCI-ESCS therapy. **b.** Corticospinal excitability measured via motor evoked potentials (MEPs). Left: Representative MEP waveforms from the extensor carpi radialis (ECR) and flexor carpi radialis (FCR) muscles at different stimulus intensities before and after therapy. Right: Boxplots of MEP amplitudes, showing significant increases in corticospinal excitability after BCI-ESCS therapy, with values returning to Pre at Follow-up. **c.** Reaching kinematics. Reaching trajectories for Pre, Post, and Follow-up assessments, showing movement refinement after therapy. Boxplots of velocity peaks, target error, and initial direction angle showing improved movement smoothness and endpoint accuracy at Post, with partial retention at Follow-up for some targets, and a persistent increase in initial direction angle. **d.** TRI-HFT performance. Radar plots show improvements in the 10-object manipulation task and the rectangular block tasks after therapy, with gains sustained at Follow-up. Boxplots compare participant's scores to those of a control cohort (n=2: C5–C6

complete and n=4: C4–C7 incomplete SCI) who underwent conventional therapy only. **e.** GRASSP (Quantitative Prehension Test). Radar plots indicate improvements in water bottle, jam jar, and coin tasks at Post, with most enhancements sustained at Follow-up. In each box plot, the central line indicates the median, the box represents the interquartile range (25th to 75th percentile), and the whiskers extend to the full range of the data (minimum to maximum). Outliers are plotted individually as additional circles. Statistical inference was performed using a bootstrap method (n=10,000 resamples) for datasets with n=5 (MEP), n=8 (reaching kinematics), or n=6 (TRI-HFT) observations per condition. Asterisks indicate statistical significance and rejection of the null hypothesis of no difference with a 95% CI.

3. Discussion

This first-in-human study provides proof-of-concept evidence that an implantable, intention-driven ESCS can promote both immediate and sustained therapeutic improvements in upper-limb motor function, even in an individual with chronic, complete cervical SCI (AIS A). Three main findings emerge. First, BCI-ESCS provided substantial assistive effects, improving grip force, reaching performance, and object manipulation compared to no stimulation (Fig. 2), consistent with improvements reported during continuous stimulation[12,13]. Second, BCI-ESCS produced rapid facilitation of corticospinal excitability within single sessions (Fig. 3), whereas tonic stimulation yielded no potentiation, underscoring the importance of volitional engagement and temporally coordinated stimulation for enhancing neuromodulatory efficacy[11,19,20,27,28]. Third, repeated BCI-ESCS therapy over the 28-day intervention revealed enhanced corticospinal excitability and meaningful functional improvements exceeding conventional therapy benchmarks (Fig. 4), with both TRI-HFT and GRASSP scores surpassing the respective MDC. These findings demonstrate the feasibility and suggest therapeutic potential of an implantable BCI-ESCS system as a neuromodulation approach for the restoration of upper-limb volitional control in individuals with severe paralysis.

In chronic complete SCI, corticospinal transmission is profoundly disrupted, and voluntary movement is typically absent below the injury level[35] (Supplementary Fig. 1). Nonetheless, our results demonstrated that both BCI-triggered and tonic cervical ESCS immediately improved grip strength, reaching trajectory, and object manipulation (Fig. 2), as also readily observed during therapy, extending previous reports of assistive effects with tonic spinal stimulation[5,6,12,13,36]. At a mechanistic level, these assistive effects arise from ESCS recruitment of primary afferents in the dorsal roots, which transsynaptically activate motoneurons and interneurons within the spinal cord[10,17,37,38], bringing their membrane potential closer to the firing threshold[5,10,39,40]. As a result, these neurons become more responsive to any residual descending cortical input, effectively lowering the activation threshold for volitional control. Although both BCI-ESCS and Tonic-ESCS can acutely enhance motor function in this individual with motor-complete SCI, BCI-ESCS may provide additional benefit immediately when the stimulation is triggered, particularly in hand grip MVC (Fig. 2a) and reaching movement initiation (Fig. 2c). Both paradigms engage the same afferent pathways; however, BCI-ESCS delivers stimulation in an intention-triggered manner, coupling stimulation onset to detected motor intent rather than providing continuous stimulation. This strategy mirrors previous approaches in non-human primates and other clinical BCI systems that have improved motor output via closed-loop intention-driven stimulation[14,18–20,41,42]. By coupling the spinal activation to the user's volitional drive, BCI-ESCS may strengthen functional coupling between cortical activity and spinal circuits, supporting facilitation of corticospinal and other residual pathways for recovery of voluntary motor function after SCI[43–46].

Beyond providing immediate assistance, BCI-ESCS induced rapid potentiation of corticospinal excitability following single sessions (Fig. 3b) and after four weeks of therapy (Fig.

4b). This finding is especially significant given that tonic ESCS does not potentiate the MEPs, suggesting that the continuous mode of stimulation is suboptimal to engage activity-dependent plasticity mechanisms. These findings align with prior evidence that intention-driven neuromodulation can enhance neuroplasticity more effectively[27,28,47], and are consistent with a Hebbian-like framework, in which repeated temporally coordinated cortical and spinal activation reinforces synaptic efficacy across spared corticospinal connections[48,49]. While our system does not control millisecond-level timing required for single-pulse paired associative stimulation that leverages spike-timing-dependent plasticity (STDP)[39,50], we demonstrate that repeated temporally synchronized activation of the motor cortex and subsequent exogenous spinal circuit activation provide conditions to drive activity-dependent synaptic plasticity to elicit long-term potentiation (LTP)-like excitability of the corticospinal tract[42]. Specifically, repeated coupling of endogenous cortical activity with stimulation-induced excitation of spinal interneurons may promote synaptic strengthening, increase excitatory drive within spinal circuits, and promote latent descending pathways. These mechanisms are consistent with the findings in rodent models, where brain-controlled stimulation induced more robust motor recovery following spinal contusions compared to continuous stimulation[49].

The Pre-to-Post increase in MEP amplitude after the four weeks of BCI-ESCS therapy suggests a cumulative, training-induced effect, which likely contributed to function restoration[43–46]. While direct evidence of anatomical change could not be investigated in humans, recent studies indicate that long-term activity-dependent stimulation can also promote circuit reorganization and even potentially axonal sprouting[51], raising the possibility that both synaptic and structural plasticity contributed to the effects we observed. These physiological improvements in corticospinal excitability translated to meaningful functional gains, with both TRI-HFT and GRASSP scores exceeding the MDC (Fig. 4d, e) alongside improvements in reaching smoothness, accuracy, and muscle coordination (Fig. 4c; Extended Data Fig. 2). Notably, gains in object manipulation and blocks of the TRI-HFT, accomplished with just 19 BCI-ESCS sessions across 4 weeks, surpassed the mean improvements in a control group that underwent 40 sessions of conventional activity-based therapy over 16 weeks (Fig. 4d). At one month follow-up without ongoing stimulation, these functional gains persisted despite MEP amplitudes returning to baseline, suggesting partial consolidation of function mediated by integrated activity across multiple neural systems operating at different timescales, rather than being solely determined by corticospinal excitability[43]. Performance improvements likely also reflect contributions from residual pathways such as the reticulospinal tract[45], spinal circuit excitability[6], and reorganization of propriospinal networks[52]. This enhanced upper-limb motor performance observed with BCI-ESCS therapy underscores the therapeutic advantage of volitional neuromodulation, wherein stimulation is temporally aligned with motor intent, thus reinforcing task-specific descending pathways. The functional gains we demonstrated in an individual with motor complete (AIS A) SCI may also exceed those of individuals with incomplete SCI after multi-week tonic stimulation protocols[12,53–55]. While direct comparisons between BCI-ESCS and tonic stimulation remain to be fully established, BCI-ESCS elicits enhanced potentiation of corticospinal excitability compared to the tonic stimulation mode (Fig. 3b). Although a controlled comparison between BCI-ESCS and tonic stimulation is warranted in future investigations, clinically meaningful improvements achieved here in a participant with motor-complete SCI underscore the therapeutic potential of intent-driven neuromodulation.

Alongside the functional improvements with BCI-ESCS therapy, the participant expressed positive sentiment around moving his upper extremities and the desire for a more permanent

solution, providing an encouraging first account of this novel therapeutic approach. Extending the duration of therapy may further enhance recovery, potentially enabling improvements in independence and quality of life beyond the four-week intervention period. Moreover, the future clinical utility of BCI-ESCS may be substantially enhanced by combining it with complementary therapeutic strategies. Combinatorial approaches that integrate neuromodulation with activity-based training and pharmacological agents such as 4-aminopyridine have recently demonstrated synergistic potential to improve functional recovery following SCI[56]. Similarly, cell-based therapies that promote tissue repair and axonal regeneration following SCI[57] may be further potentiated by spinal neuromodulation to support enhanced functional restoration. Therefore, combining activity-dependent stimulation with regenerative interventions may provide a multimodal framework for promoting axon regeneration and circuit reorganization following SCI[51]. Overall, our BCI-ESCS neuromodulation approach represents a shift in the role of brain-computer interfaces, from assistive prosthetic approaches to therapeutic tools that could effectively harness volitional intent to drive synaptic neural plasticity. This mechanistically distinct approach enables targeted, activity-dependent neuromodulation that promotes functional recovery even following chronic complete SCI, offering a promising new direction for restorative neurorehabilitation.

This study presents a first-in-human proof-of-concept investigation, and therefore the generalizability of the findings should be interpreted with limitations. Longitudinal corticospinal excitability was assessed at three time points (Pre, Post, and Follow-up) on single days, precluding full characterization of neurophysiological fluctuations. Nevertheless, the MEP potentiation observed following BCI-ESCS therapy (Fig. 4b) aligns with prior evidence that intention-driven neuromodulation can induce activity-dependent plasticity[11,19,20,27,28]. The short-term effects were assessed in two sessions per condition (BCI-ESCS and Tonic-ESCS) using an interleaved crossover design to minimize order effects and state-dependent variability. However, recruitment curves obtained from single-participant recordings may exhibit non-monotonic patterns across stimulation intensities, and additional repeated assessments in larger cohorts will be important to further characterize these effects. Consistent findings across assistive (Fig. 2), single-session (Fig. 3), and longitudinal (Fig. 4) measures provide converging early evidence that BCI-ESCS could potentiate corticospinal excitability and motor function. Additionally, we acknowledge that false positive rates could not be explicitly computed during real-time BCI operation. The BCI system achieved a success rate of approximately 84%, comparable to previous work using a similar decoder architecture that reported a chance level of 34% (i.e., the detection rate during passive rest)[27,28]. Given that the success rate substantially exceeds this chance level, BCI performance is expected to reflect reliable ERD activity at stimulation onset, consistent with activation patterns observed during calibration (Section 4.5).

4. Methods

4.1. Trial and participant information

The study was approved by the University of Miami Institutional Review Board (IRB) (IRB 20190536) and conducted in accordance with the Declaration of Helsinki. The experimental protocol for this study is registered on ClinicalTrials.gov (NCT06533969).

Participant information. One individual participated in this study after providing written informed consent. The participant was a male in his 20's with a history of traumatic C4–C5 SCI (AIS A), who had undergone anterior cervical discectomy and fusion (C3–C5) in 2015. In 2018,

the participant first underwent implantation of an ECoG-based BCI device over the motor cortex as part of a separate clinical trial (NCT02564419)[22,23].

The participant was recruited based on the following inclusion criteria: medically stable adult (>18 years old) with chronic (>6 months) traumatic SCI at the C4–C6 level and some residual motor function. Exclusion criteria for the study included contraindications to spinal cord stimulation (e.g., wounds near the stimulation site, muscle denervation, unmanaged autonomic dysreflexia, recent botulinum toxin injections), contraindications to cortical stimulation (e.g., history of epilepsy/seizures), or surgical ineligibility for ESCS (e.g., unfavorable spinal anatomy, anticoagulation therapy, neurological conditions unrelated to SCI, pregnancy).

Study design and data reported. This single-case pilot study aimed to assess the therapeutic potential of BCI-ESCS therapy in enhancing upper-limb motor function in chronic SCI. A total of 19 therapy sessions were completed over four weeks (28 days) following ESCS lead implantation. Each therapy session lasted approximately 40 minutes and included at least three motor tasks, each performed for 10 to 30 minutes. Over the four-week period, the participant completed a total of 16 BCI-ESCS sessions and 3 Tonic-ESCS sessions enabling comparison of different stimulating modes with a major focus on longitudinal therapeutic effects. The study outcomes focused on evaluating assistive effects (stimulation on/off), short-term effects (pre-post single session), and longitudinal therapeutic effects (recovery of voluntary function).

During therapy sessions, we investigated the assistive and short-term effects of BCI-ESCS compared to Tonic-ESCS therapy. The assistive effects were assessed on separate days for each condition by evaluating motor function under three different stimulation conditions: no stimulation, Tonic-ESCS, and BCI-ESCS. Assessments included maximum grip force measured during MVC (two trials per condition), selected TRI-HFT subtests involving the manipulation of a mug, mobile phone, dice, and rectangular blocks, as well as performance in a 3D reaching task.

The single-session effects were assessed in an interleaved crossover design with two sessions for each BCI-ESCS and Tonic-ESCS condition (Tonic-ESCS: days 6 and 22 post-implant; BCI-ESCS: days 10 and 21 post-implant; Supplementary Fig. 2) to mitigate potential order effects. Both sessions were matched across conditions for session duration, number of training trials, and training tasks. All sessions were conducted at the same time of day to reduce potential variability related to fatigue and spasticity. To evaluate these effects, neurophysiological assessments, including corticospinal excitability measured through motor evoked potentials (MEPs) and spinal excitability measured through posterior root muscle (PRM) reflexes, were conducted before and after each 28-minute therapy session. Additionally, functional motor performance was evaluated using the 9HPT and the BBT due to their sensitivity to subtle motor changes over short timeframes.

To assess longitudinal effects, evaluations were conducted at three time points: prior to implantation (Pre), after the therapy period (Post), and one month following lead explant (Follow-up). The primary outcome measure was functional improvement assessed using the TRI-HFT. Secondary outcomes included changes in the GRASSP scores, neurophysiological measures of corticospinal excitability, kinematics and muscle synergies during a 3D reaching task, qualitative assessments of pain, quality of life (QoL), and levels of independence. Additionally, spasticity was evaluated before each therapy session, and the International Standards for Neurological Classification of Spinal Cord Injury (ISNCSCI) was administered at baseline for participant screening and at follow-up for efficacy evaluation.

4.2. Surgical procedure

Prior to surgery, the participant underwent pre-operative screening, including laboratory tests, imaging, prophylactic antibiotics, and a thorough discussion with the research and medical teams over the risks involved. Pre-operative imaging included a non-contrast computed tomography (CT) scan of the head, cervical, and thoracic spine. The ESCS system required temporary surgical placement of two eight-contact percutaneous leads (PN 977A260, Medtronic) in the epidural space of the spinal cord for 28 days, after which the same surgical team removed the leads. During surgery, the participant was placed under general anesthesia, and a head fixation device stabilized the participant's head and neck. A short cephalocaudal incision was made along the upper thoracic spine midline, and an epidural needle was inserted under fluoroscopic guidance into the interlaminar space, leveraging evidence that rostral entry points minimize displacement[58]. Both leads were placed unilaterally on the right side, with the most rostral tips of the leads placed just caudal to the level of injury, just below the C5 vertebrae, with the lateral lead more rostral than the medial lead by one contact (Fig. 1). Lead positioning was guided by intraoperative fluoroscopy and electrophysiological feedback of muscle action potentials, ensuring selective recruitment of ipsilateral motor pools[13]. During this monitoring, the lead was temporarily connected to the intraoperative monitoring system (Natus XLTEK Protektor 32) via 60 cm extensions (PN 3708160, Medtronic), which were removed after testing. The leads were then anchored to the fascia and tunneled subcutaneously to a distant counter incision where the extension leads were externalized for use in later stimulation procedures coupled with neural signal recordings. Percutaneous leads were removed 28 days after implantation under monitored anesthesia care by reopening the cephalocaudal incision and releasing the anchors.

4.3. Electromyography acquisition system

Post-operatively, EMG signals were recorded from the right deltoid (DEL), biceps brachii (BB), triceps brachii (TB), ECR, FCR, abductor digiti minimi (ADM), abductor pollicis brevis (APB), and first dorsal interosseous (FDI) muscles. The skin was prepared using disposable razor blades and alcohol swabs before placing bipolar surface EMG electrodes (Ag/AgCl, H124SG, Kendall) over each muscle belly, as well as ground electrodes over the ulnar styloid process and the lateral epicondyle. All signals were amplified (×1,000), band-pass filtered (15–1,000 Hz) using bio-amplifiers (D360R, Digitimer), and digitized (4,000 Hz) with an analog-to-digital converter (Power 1401, Cambridge Electronic Design). EMG activity was recorded during the ESCS spinal mapping session (Section 4.4) and neurophysiological assessment (Section 4.10).

4.4. Epidural spinal cord stimulation (ESCS) system

ESCS was administered using a constant current electrical stimulator (DS8R, Digitimer), as well as a multiplexer (D188, Digitimer) and a custom-built control unit to regulate the pulse timing, amplitude, and output channel selection[13] (Fig. 5). To interface the stimulator with the percutaneous lead, the system was connected to an accessory kit (355531, Medtronic) via a Medusa electrode cable (Threshold NeuroDiagnostics). The percutaneous lead served as cathode electrodes, and a 2x4" anode electrode (Natus) was placed over the left (contralateral) iliac crest. Each stimulation pulse was set as a symmetrical biphasic waveform with a 200 µs pulse width and 10 µs interphase interval (Fig. 6).

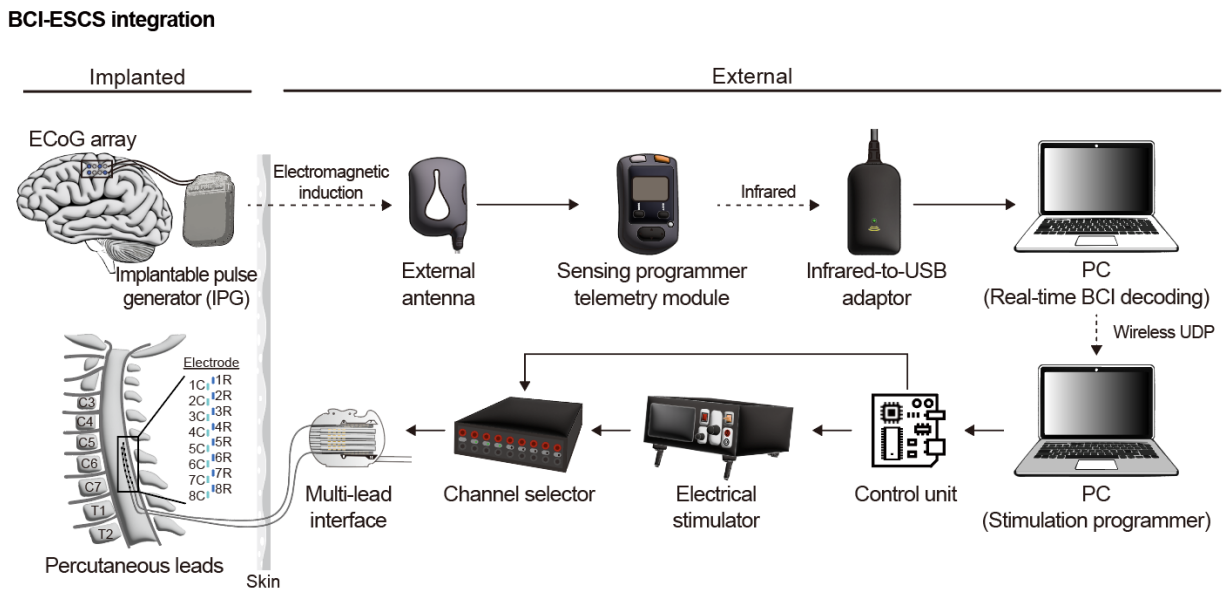

Fig. 5: BCI-ESCS system integration | Schematic representation of the brain-computer interface (BCI)-controlled epidural spinal cord stimulation (ESCS) system, illustrating the interaction between implanted and external components. The implanted system consists of an electrocorticography (ECoG) array connected to an implantable pulse generator (IPG), which was used for ECoG signal acquisition (and for single-pulse motor cortex stimulation to elicit motor evoked potentials; see Section 4.10). ESCS was delivered via an external constant-current stimulator (Section 4.4). Separately, percutaneous epidural leads are implanted in the cervical spinal cord to deliver ESCS. Neural signals from the ECoG array are transmitted wirelessly via an external antenna through electromagnetic induction to a sensing programmer telemetry module, which relays the data to a PC for real-time BCI decoding. Upon detection of motor intent, a control unit processes the decoded signals and triggers the electrical stimulator via a channel selector, directing current through the percutaneous leads to selectively activate optimized channels. Stimulation parameters are managed through a separate PC interface, allowing precise control of pulse timing and amplitude. This implantable BCI-ESCS system enables real-time, intention-driven spinal modulation to restore volitional upper limb movement in individuals with SCI.

Segment-level muscle recruitment. Using intraoperative fluoroscopy as an initial anatomical reference (Supplementary Fig. 6), we conducted a spinal mapping session within the first days post-implant to determine segment-level muscle recruitment profiles. Muscle recruitment curves were generated by applying paired-pulse stimulation with a 50-ms interstimulus interval[59,60]. For each contact, the stimulation intensity was gradually increased from 0 mA until evoked responses were observed in all right-hand muscles or any contralateral (left) effects. Stimulation intensity did not exceed 6.2 mA. From the recruitment curves, we identified contacts and stimulation intensities that produced selective muscle activation via the innervation of primary afferent fibers (Fig. 6), as indicated by post-activation depression in the second responses[59,60]. These identified contacts and intensities served as references for subsequent therapy sessions, with brief spinal mapping assessments conducted before each session to verify stable recruitment. Given that deviations in recruitment patterns were observed during pre-therapy verification on day 7 post-implant, we repeated complete spinal mapping and acquired additional cervical plain radiography (Supplementary Fig. 6) to verify anatomical position and re-optimize stimulation parameters. Consequently, we updated optimal contacts for functional tasks such as reaching (shifted from 4R to 3R) and grasping (shifted from 5R to 4R) (Supplementary Fig. 2), corresponding to the lead displacement (Supplementary Fig. 6). Daily spinal mapping verification in subsequent days

confirmed stable recruitment profiles throughout the remainder of therapy (Weeks 2-4), which aligns with prior evidence showing minimal lead displacement after the second week[13].

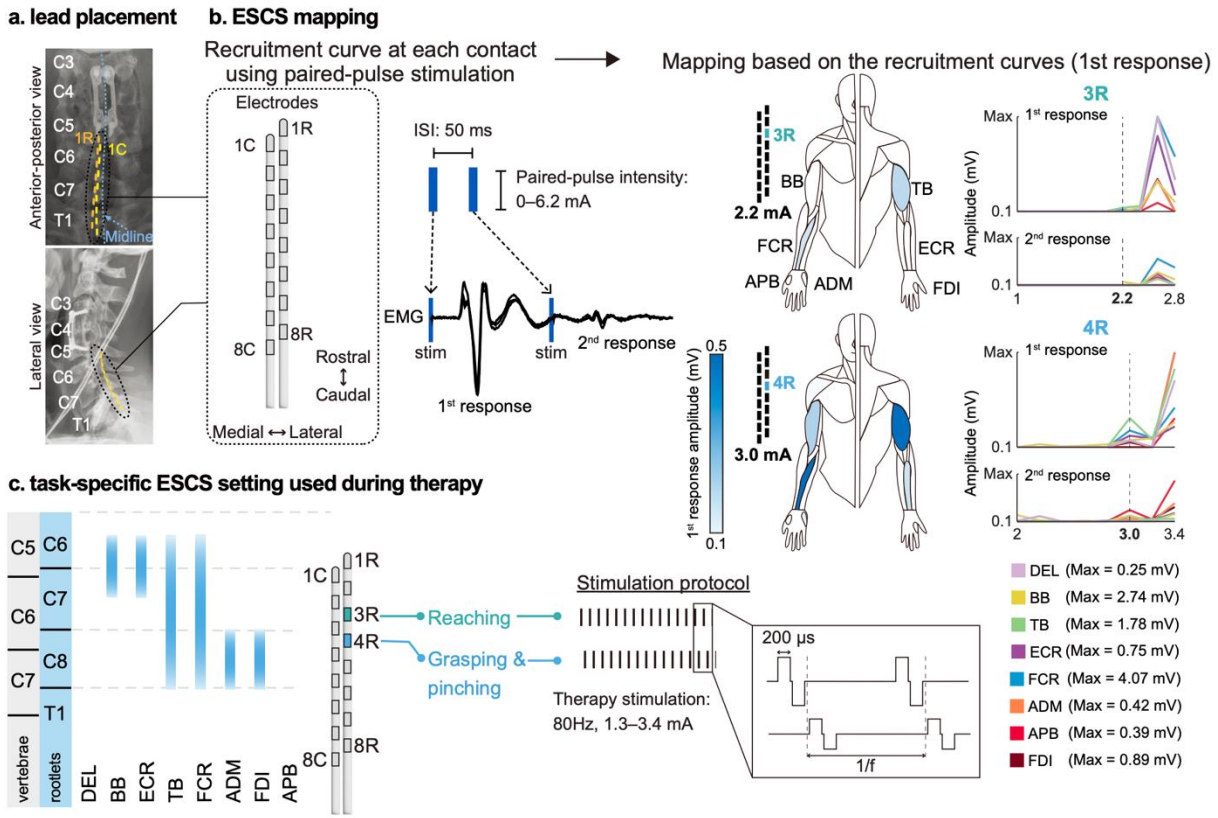

Fig. 6: ESCS lead placement and spinal mapping for muscle recruitment | a. Lead placement: Post-operative X-ray images showing the positioning of the percutaneous epidural spinal cord stimulation (ESCS) leads at the cervical spinal cord. The leads were implanted over the dorsal roots at C6–T1 to selectively target upper-limb muscles. **b.** ESCS mapping: Recruitment curves were obtained by applying paired-pulse stimulation (interstimulus interval [ISI]: 50 ms) at increasing intensities (0–6.2 mA) to each contact. EMG recordings were used to assess evoked muscle responses. Recruitment curves for contacts 3R and 4R illustrate muscle-specific activation patterns, with the second response showing post-activation depression, confirming activation via primary afferent fibers. **c.** Optimal ESCS settings for continuous stimulation: Stimulation parameters were optimized to selectively modulate reaching, grasping, and pinching movements, with stimulation intensities ranging from 1.3 to 3.4 mA at 80 Hz and a biphasic pulse width of 200 µs. These settings ensured targeted muscle activation while minimizing unintended co-contraction.

ESCS optimization for therapy sessions. For each therapy task, ESCS contacts were selected based on segment-level muscle recruitment mapping, with stimulation parameters (frequency and intensity) optimized to maximize support during volitional movements while preventing involuntary muscle twitching. Specifically, stimulation contacts that innervated the upper arm were selected for reaching tasks and contacts that innervated the forearm and fingers were selected for grasping and pinching tasks (Fig. 6). At the beginning of each therapy session, stimulation contacts were adjusted to ensure optimal neuromodulation, and alternative contacts were used if necessary to enhance motor performance (Supplementary Fig. 2). For each selected contact, stimulation frequencies ranging from 40–100 Hz were tested[13], with 80 Hz identified as optimal for maximizing assistive benefits. Stimulation intensities were set using a functional, task-

based criterion, and titrated to facilitate volitional movement while remaining below the level that produced overt movement at rest[6,13], which were near or just below the motor threshold to elicit PRM reflex responses. The intensities were marginally adjusted throughout therapy, ranging from 1.3 to 3.4 mA.

4.5. BCI system

ECoG acquisition system. Cortical activity was recorded using two four-contact electrodes (Resume II Leads, Medtronic) implanted over the sensorimotor cortex's hand knob region during previous clinical trials[22,23] (Fig. 7). These electrodes were subcutaneously connected to an implanted pulse generator (IPG) (Activa PC+S, Medtronic) that enables the recording of two bipolar time-series channels (Ch 0-3 and Ch 8-10) (Fig. 5). In this study, the IPG was used for ECoG signal acquisition to support real-time BCI decoding. Single-pulse motor cortex stimulation delivered via the IPG for MEP assessment is described in Section 4.10. The acquisition system applied a 0.5-100 Hz band-pass pre-amplifier filter and sampled data at 200 Hz, with an internal buffer of 400 ms[61].

BCI decoding. The BCI system was adapted from previous studies[24–28] to detect motor imagery of hand movements (Fig. 7) by analyzing real-time changes in ECoG signal power. This signal was then used to trigger continuous ESCS during activity-based therapy (see Section 4.6).

Before therapy (baseline), a BCI calibration session was conducted to determine the optimal channel and frequency. During this session, the participant performed 10 motor imagery trials for each of the following movements: reaching, grasping, supination, pronation, lateral pinching, and pulp pinching. From these 60 total trials, time-frequency spectrograms were computed to identify the optimal ECoG channel (Ch 0-3) and frequency range (8-14 Hz) exhibiting the strongest event-related desynchronization (ERD) during motor imagery tasks[25–28] (Fig. 7). These calibrated features were subsequently used for BCI decoding of all motor imagery tasks.

To decode motor imagery during BCI-ESCS therapy, a one degree-of-freedom classifier was developed to detect a transition between rest and active motor imagery state[24–28]. A single decoder was used across all motor imagery tasks, such that activation of stimulation could be achieved by imagining any of the trained movements. Decoding was based on ERD activity from the calibrated channel (Ch 0-3) and frequency band (8-14 Hz) identified during the baseline BCI calibration session (Fig. 7a). For each trial, video cues (Fig. 7b) instructed the participant on the specific task to guide task execution during therapy. Specifically, the BCI system acquired ECoG signals from the selected channel and applied a band-pass filter within the calibrated frequency range. The root-mean-square (RMS) value of the filtered signal was computed every 100 ms and subsequently smoothed using a 1-second moving average window to obtain the signal power. To trigger continuous ESCS, the BCI system monitored the ECoG signal power within a 15-second window after the participant was instructed to imagine the corresponding task (i.e., Go cue, Fig. 7). If the signal power remained below a predefined threshold for at least one second[24–28], the BCI system triggered ESCS for a task-specific, pre-programmed duration (4–25 s) to assist the participant in performing the corresponding activity-based therapy task. At the end of this stimulation window, ESCS automatically returned to the off state and remained off until the next trial. The threshold was determined prior to each therapy session during a practice period. The experimenter adjusted the signal power level to distinguish rest from motor imagery states initially with the level readjusted periodically throughout sessions as needed to compensate for drift[24–28]. Conversely, if motor imagery was not detected, ESCS was not triggered, and the participant remained at rest before proceeding to the next task. BCI performance was quantified as the success rate, calculated as the proportion of detected motor imagery (i.e., successful trials) out of the total number of trials,

resulting in a mean success rate of 83.8±4.2%. This success rate remains stable across therapy sessions (Spearman rank correlation between session number and success rate: $\rho \approx 0$, $p > 0.999$, df=14), with no significant differences found across motor tasks (Kruskal-Wallis test: H(5)=0.757, p=0.980).

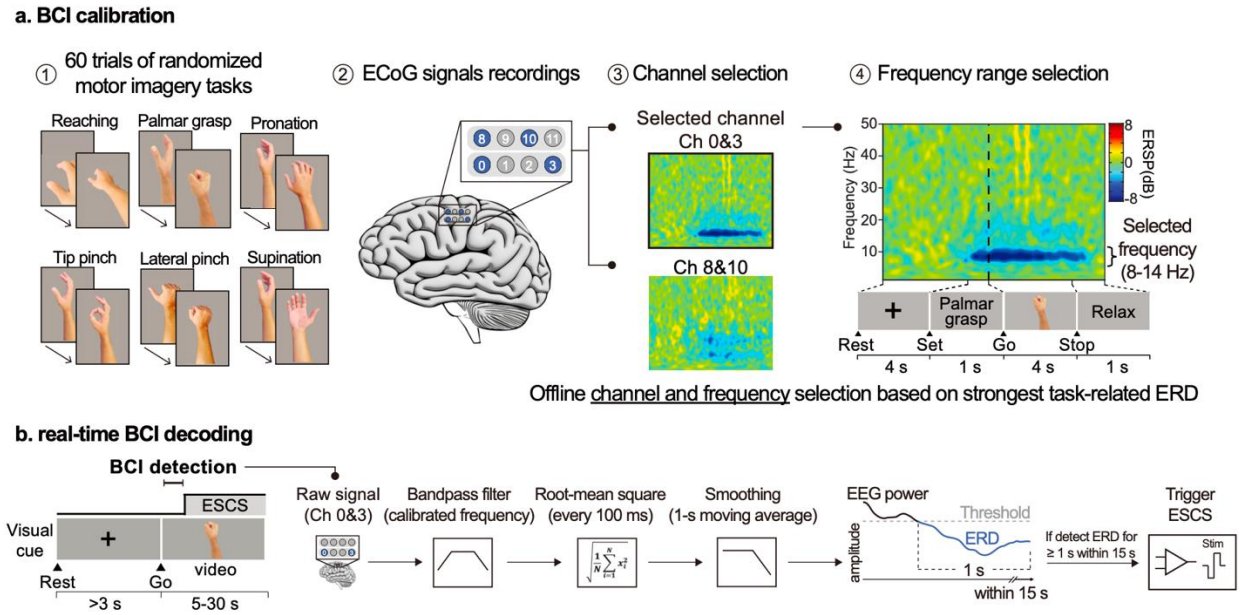

Fig. 7: BCI calibration and real-time decoding for BCI-ESCS therapy | a. BCI calibration process. The participant performed 60 trials of randomized motor imagery tasks, including reaching, palmar grasp, pronation, tip pinch, lateral pinch, and supination. ECoG signals were recorded from implanted electrodes, and offline analysis was conducted to determine the optimal ECoG channel and frequency range based on event-related desynchronization (ERD). Channel selection was performed by comparing activation patterns across electrodes, and the frequency range (8-14 Hz) was selected based on the strongest task-related ERD. **b.** Real-time BCI decoding during therapy. Raw ECoG signals from the selected channels (Ch 0 and Ch 3) were processed in real-time using a band-pass filter (calibrated frequency) and converted into a root-mean-square (RMS) value every 100 ms. A 1-second moving average smoothing was applied to track signal power. If the ECoG power remained below a predefined ERD threshold for at least one second within a 15-second window, the BCI system triggered ESCS to support the intended movement.

4.6. BCI-ESCS therapy protocol

The therapy was conducted by a physical therapist and two BCI-ESCS operators, focusing on restoring right-hand upper limb function through activity-based training with BCI-triggered ESCS. The physical therapist guided the participant through a series of motor tasks, while the BCI system continuously monitored motor imagery and triggered ESCS in real-time to facilitate volitional movement.

At the start of each task, a visual cue corresponding to the intended movement (e.g., reaching, grasping, pronation, supination, lateral pinching, and pulp pinching) was presented on a monitor (Fig. 8). Upon receiving the "Go" cue, the participant attempted the motor imagery. When motor imagery was detected (see Section 4.5), the BCI system triggered ESCS, providing stimulation to enhance movement execution. If necessary, the therapist provided minimal assistance to the upper limb, thereby enabling the participant to move in the intended direction with voluntary effort and less compensation.

To progressively enhance motor function, task difficulty was adjusted throughout the intervention. Initially, the participant engaged in simple isolated movements (e.g., reaching or

grasping). As performance improved, more complex combination tasks (e.g., reaching and grasping simultaneously) were introduced (Fig. 8d). Training was further enriched using objects of varying weight, size, and texture (e.g., cups, blocks, balls) to enhance sensorimotor engagement. Additionally, task parameters such as movement height and distance were modified to challenge motor control. In later stages of therapy, the participant practiced functional movements relevant to daily living, such as mimicking drinking or eating, to promote practical skill acquisition.

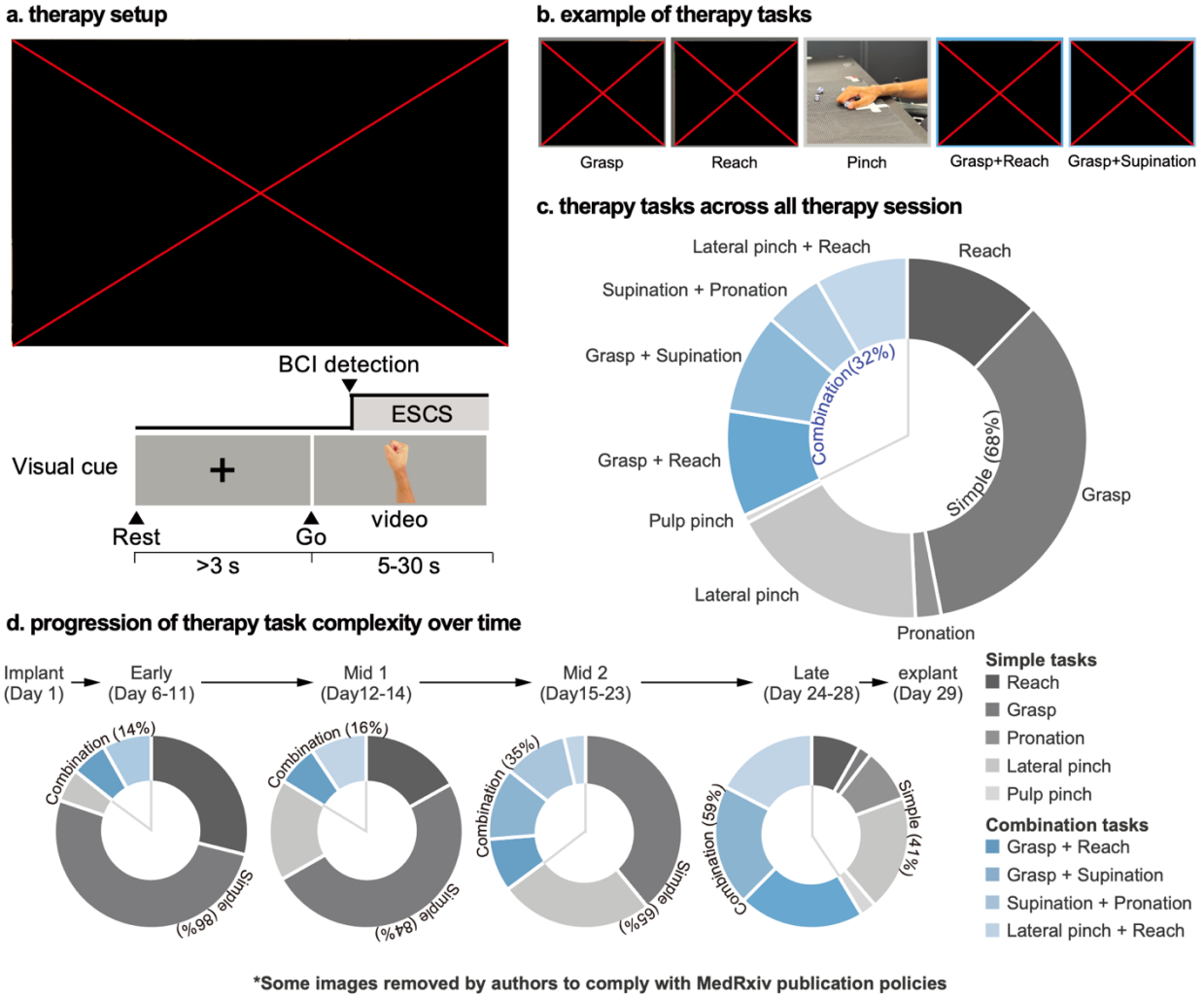

*Some images removed by authors to comply with MedRxiv publication policies

Fig. 8: BCI-ESCS therapy setup and task progression over long-term intervention | **a.** Therapy setup: The participant sat in a wheelchair facing a monitor displaying visual cues corresponding to the instructed motor tasks. Upon receiving the "Go" cue, the participant attempted the motor imagery while the BCI system detected motor intention and triggered ESCS in real time. The stimulation remained active throughout the task execution phase. **b.** Examples of therapy tasks. The participant engaged in functional hand and arm movements, including grasping, reaching, pinching, and combined movements such as grasp + reach and grasp + supination, mimicking real-life functional tasks. **c.** Task distribution across all therapy sessions. Throughout the four weeks (28-day) therapy period, the participant performed a variety of motor tasks, including simple isolated movements (e.g., reaching, grasping, pronation, supination, lateral pinching, pulp pinching) and complex combination movements (e.g., grasp + reach, grasp + supination, supination + pronation). Simple movements accounted for 68% of total tasks, while combination movements comprised 32%, reflecting a progressive increase in task complexity aimed at improving functional motor coordination. **d.** Progression of therapy task complexity over time. The proportion of combination tasks increased throughout the four-week therapy period. Initially, simple tasks dominated the

sessions (86% early on), but as therapy progressed, the participant performed a greater proportion of complex combination tasks, reaching 59% by the final sessions.

4.7. Tonic-ESCS as a control for assistive and short-term effects

Tonic-ESCS was implemented as a control condition to evaluate the assistive and short-term (single session) effects of BCI-ESCS therapy. During the Tonic-ESCS condition, stimulation was delivered continuously (without the BCI trigger) throughout the session. Stimulation parameters were optimized before each task, following the same procedure as in the BCI-ESCS condition, ensuring that stimulation facilitated movement without excessive involuntary muscle activation.

To minimize variability, for short-term effects, the BCI-ESCS and Tonic-ESCS conditions contained equal therapy tasks and durations under the guidance of a physical therapist.

4.8. Clinical assessments

Toronto Rehabilitation Institute-Hand Function Test (TRI-HFT). The TRI-HFT is a standardized assessment of unilateral gross motor function of the upper extremity, with an emphasis on pinch and palmar grasp. It consists of two components: (1) object manipulation, in which individuals are evaluated on their ability to manipulate ten everyday objects and a set of rectangular blocks, and (2) grip strength assessment, comprising three sub-tests to measure lateral grip and palmar grasp strength[62]. We used a 3D-printed version of the TRI-HFT and focused primarily on the object manipulation component, which has been validated in individuals with SCI[63]. Each object is scored on a scale from 0 to 7, with higher scores reflecting better function.

The TRI-HFT assessments were administered by a licensed physical therapist who also served as the training therapist in this study. Potential rater bias was mitigated by having another independent rater, who was not involved in the intervention but is trained in TRI-HFT, score performance from video recordings. Any discrepancies between the two raters were resolved through discussion to reach consensus.

To assess the effects of our four-week BCI-ESCS intervention, we compared TRI-HFT outcomes to control data from six individuals with chronic SCI (n=2: C5–C6 complete and n=4: C4–C7 incomplete SCI; 5.7±3.1 years since injury) who underwent conventional activity-based therapy without neuromodulation at the Rehabilitation Engineering Laboratory (KITE Research Institute - University Health Network). The training protocol and partial dataset are described by Kapadia et al.[64], where participants completed 40 one-hour therapy sessions over 16 weeks. In contrast, the individual in our current study completed 19 sessions of approximately 40-minute BCI-ESCS therapy combined with comparable activity-based rehabilitation. The control comparison evaluated whether the TRI-HFT improvements in our participant with a motor-complete SCI exceeded those observed in the control group.

Graded Redefined Assessment of Strength, Sensibility and Prehension (GRASSP). The GRASSP is a comprehensive and sensitive measure of the upper limb impairment and function in the cervical SCI population, which was used to assess three domains of recovery: sensation, strength, and prehension[65,66].

The International Standards of Neurological Classification of Spinal Cord Injury (ISNCSCI). The ISNCSCI is a standardized classification tool for SCI used to systematically assess sensory and motor levels of injury to determine the neurological level of the injury and severity (i.e., completeness) of the SCI[67]. ISNCSCI classification at baseline and study completion was performed by the same trained assessor, whose dedicated role is to conduct standardized neurological assessments, ensuring consistency and minimizing inter-rater variability.

4.9. 3D reaching assessment: kinematics and muscle coordination

Reaching task. The participant was asked to reach forward to four targets (center, left, right, and upward targets) with varying heights and lateral positions. The center target was positioned 40 cm horizontally from the body, aligned with the right shoulder. Left and right targets were horizontally placed 20 cm to the left and right of the center, while the upward target was placed vertically 20 cm above the center. A single reaching cycle was defined as the hand moving from the initial position to the target (reaching phase) and returning to the initial position (pull phase). The reaching task was repeated eight times per target before the next target was assigned in randomized order. The participant was instructed to reach as accurately as possible at a self-selected pace without time constraints. These reaching movements differed from those used during the training sessions, minimizing the likelihood of task learning effects. We compared reaching kinematics and muscle synergies before and after four weeks of therapy sessions (i.e., longitudinal effects), and during the use of BCI-ESCS and Tonic-ESCS (i.e., assistive effects).

Kinematics. Marker trajectory data of right-hand movement were acquired and sampled at 100 Hz using a twelve-camera motion capture system (Vicon Vero, Oxford, UK). One reflective marker was placed on each of the four targets, and another marker was placed at the ulnar styloid to track the wrist trajectory. The kinematic analysis focused on reaching trajectories, velocity peaks, target error, initial direction angle, path length, and reaching time for each target. All kinematic computations were performed in 3D using the full marker trajectories. For visualization, reaching trajectories were plotted in 2D planes according to target direction: the horizontal plane for the center, left, and right targets, and the vertical plane for the upward target (Figs. 2c and 4c).

Velocity peaks were analyzed as a measure of movement smoothness, which is derived directly from the velocity profile and minimizes sensitivity to high-frequency measurement noise[13]. This metric quantified the total number of local maxima and minima in the velocity profile during both the reaching and pulling phases. Movements with a higher number of velocity peaks indicated less smooth movement, characterized by frequent accelerations and decelerations[13]. To identify these peaks, we applied a *findpeaks* function in MATLAB with a prominence threshold of 10% of the velocity profile's range. This threshold filtered out minor noise and ensured that only significant variations in velocity were captured. Target error was calculated as the 3D Euclidean distance between the wrist marker position and the corresponding target position at reaching termination. The initial direction angle was calculated as the angular deviation between the vector from the onset position to the target and the vector from the onset position to the hand position at the end of the initial movement phase, defined as the point of maximum velocity[30,68]. The calculation was performed in MATLAB using the *acos* function to determine the angle in radians, which was then converted to degrees, ensuring an objective assessment of the initial movement direction relative to the intended trajectory. Path length was calculated as the total 3D trajectory length of the wrist during the reaching phase (sum of Euclidean distances between consecutive wrist marker positions). Lastly, reaching time was defined as the time between movement onset and reaching termination.

In addition to kinematic outcomes, we quantified muscle synergies to characterize the coordination-level organization during reaching (Extended Data Fig. 2 and 3). This analysis provides a descriptive summary of how patterns of muscle co-activation and their temporal recruitment relate to reaching control and is used to complement the kinematic measures and mechanistic understanding underlying changes in movement kinematics.

4.10. Neurophysiological assessment: corticospinal and spinal excitability

Corticospinal excitability. We measured corticospinal excitability using motor evoked potentials (MEPs) of the ECR and FCR muscles elicited via subdural ECoG electrode single-pulse motor cortex stimulation (MCS) while the participant remained at rest. A voltage-regulated generator (Activa PC+S, Medtronic) delivered 450 µs long pulses in bipolar configuration, with contact 9 as the anode and contact 10 as the cathode. The IPG was used to deliver single-pulse motor cortex stimulation for MEP assessment. This contact configuration was selected based on our preliminary investigation, as it elicited MEPs in the FCR and ECR muscles at the lowest stimulation intensity compared to other combinations. We recorded MEPs using stimulation intensities ranging from 4.0 to 10.5 V, with five stimuli per intensity.

Single-session effects were assessed immediately before (Pre) and after (Post) each short-term BCI-ESCS or Tonic-ESCS intervention (Fig. 3b) using an interleaved crossover design. Assessments were conducted on days 6 and 22 for Tonic-ESCS and days 10 and 21 for BCI-ESCS (Supplementary Fig. 2). Pre-intervention MEP amplitudes did not differ between conditions at any timepoint (Supplementary Table 2), confirming that baseline excitability was comparable across conditions in both ECR and FCR muscles.

Longitudinal effects were assessed at baseline (Pre), after completion of therapy (Post), and more than one month after lead explant (Follow-up) (Fig. 4b). Additional longitudinal MEP recordings obtained from single-session Pre assessments are shown in Supplementary Fig. 4. These data reveal a progressive emergence of corticospinal potentiation: MEP amplitudes showed no changes during early phase (days 6-10), increased significantly during the late phase (days 21-22/Post), and subsequently declined toward baseline levels at Follow-up (Supplementary Fig. 4).

Spinal excitability. We evaluated posterior root muscle (PRM) reflexes of the ECR and FCR muscles elicited by paired-pulse ESCS using the 4R contact, which simultaneously induced responses in both muscles at the lowest stimulation intensity compared to other contacts. The PRM reflexes represent the transsynaptic activation by Ia sensory fibers[59,60]. We recorded PRM reflexes at gradually increasing intensity, with three paired-pulse stimuli delivered at each intensity. Spinal excitability was assessed before and after short-term interventions of BCI-ESCS and Tonic-ESCS. For the short-term crossover experiment, PRM reflex assessments were performed over two sessions per condition, and analyses were conducted on pooled data across the two sessions. Because the paired-pulse ESCS intensities differed between sessions, intensity for PRM analyses was referenced to a session-specific motor threshold (MT). Referencing PRM analyses from MT-0.4 mA to MT+0.6 mA captures a comparable physiological range of the recruitment curve spanning subthreshold levels, activation threshold, and the rising slope. MT was defined at the Pre (baseline) of each session as the lowest intensity at which the first response exceeded 0.05 mV peak-to-peak in 3 of 3 paired-pulse trials in both muscles. MT values for the first session were BCI: 3.0 mA and Tonic: 2.4 mA; for the second session, BCI: 2.4 mA and Tonic: 2.2 mA.

4.11. Qualitative assessments: pain, quality of life, and independence assessments

The International Spinal Cord Injury Pain Basic Data Set (ISCIPBDS) version 2.0. The ISCIPDS version 2.0 was developed to collect a minimal amount of standardized information necessary for determining interference of pain with physical and emotional function and sleep, probable pain diagnosis, location, intensity and duration[69].

The International Spinal Cord Injury Quality of Life Basic Data Set (QoL-BDS) version 2.0. The QoL-BDS version 2.0 consists of four items for individuals to rate their satisfaction with life as a whole, physical health, psychological health, and social life[70,71].

Spinal Cord Independence Measure-Self Care (SCIM-SC) III. The SCIM III is the comprehensive ability rating scale for individuals with spinal cord injury that consists of three principal areas of daily living function: self-care, respiration and sphincter management, and mobility[72,73]. This study specifically focused on the domain of self-care, which includes feeding, bathing, dressing, and grooming.

4.12. Hand dexterity assessments

Nine-hole Peg Test (9HPT). The 9HPT was used to assess finger dexterity following neurological injury[74,75]. The participant was instructed to pick up the pegs one at a time and place them in the holes as quickly and accurately as possible. Since the participant could not complete the test, the number of pegs successfully placed in 50 seconds was counted.

Box and Block Test (BBT). The BBT measures manual dexterity by counting the number of wooden blocks (2.5 cm each) that a participant can transport from one side of a box to the other within 60 seconds, typically in individuals with central paresis[76,77]. Participants are instructed to place their hand on the table beside the box. Upon the examiner's cue to begin, they reach into the box and move one block at a time across a central partition to the opposite side, repeating the action as many times as possible within the allotted time. Only blocks that fully cross the divider are counted toward the final score, and only one block may be moved at a time.

4.13. Spasticity assessment

Modified Ashworth Scale (MAS). The MAS was conducted to evaluate muscle spasticity, using a rating of muscle resistance on a 0–4 ordinal scale[78], before and after each ESCS therapy session. Assessments were performed on the right upper limb, targeting the shoulder flexor muscles and both extensor and flexor muscle groups of the elbow, wrist, and fingers. These repeated evaluations enabled close monitoring of potential spasticity changes related to the intervention.

4.14. Safety

The study was designed to prioritize participant safety, with continuous monitoring by a multidisciplinary team of neurosurgeons, physical therapists, and medical staff. Post-operatively, we conducted daily wound care. A standard post-operative dressing was applied over the cephalocaudal incision, which was sealed with surgical glue, and changed at least five times per week. A silver-infused antimicrobial barrier wound dressing (Silverlon Island Dressing ID-46) was applied over the extensions that exited from the participant's back and changed approximately every three days[13]. There was no evidence of infection at the lead exit sites.

All adverse events were recorded, reported to the IRB, and managed by the medical team. There were no serious adverse events reported during the study, and none were related to the BCI-ESCS intervention. The participant experienced a urinary tract infection during the study that was promptly treated and determined by the study team and the IRB to be unrelated to study procedures. We also did not observe any autonomic dysreflexia episodes, and overall vital signs (blood pressure, heart rate, and oxygen saturation) remained stable throughout the study. A post-session drop in blood pressure was observed during the early therapy sessions (Supplementary Fig. 7), which was determined by the study team to be most likely due to changes in posture during prolonged upright sitting. Furthermore, improvement in motor function (ISNCSCI in Supplementary Table 7, TRI-HFT in Extended Data Table 1, and GRASSP scores in Extended Data Table 2) suggests the absence of neurological deterioration. Spasticity (Supplementary Fig.

8) and pain levels (Supplementary Table 10) also remained stable, with no signs of deterioration or relief, suggesting that the intervention did not negatively influence these outcomes.

4.15. Statistics

Statistical comparisons were performed using a bootstrap method[13]. This approach was applied to assistive effects (between-condition), short-term effects (within-condition and between-condition), as well as longitudinal changes, including single-case comparisons against a control cohort. With 10,000 bootstrap iterations, we obtained a distribution of mean differences, and a 95% confidence interval (CI) was derived[13]. Statistical significance was determined by rejecting the null hypothesis of no mean difference if the 95% CI did not include zero. Where multiple comparisons were conducted, Bonferroni correction was applied to adjust the p-values accordingly. For the assistive effects, functional outcomes were analyzed between conditions (no-stim, Tonic-ESCS, and BCI-ESCS). For the single-session effects, neurophysiological outcomes were analyzed within a three-factor design comprising condition (BCI-ESCS, Tonic-ESCS), timepoint (Pre, Post), and stimulation intensity. Analyses included condition × timepoint effects (i.e., across all intensities) and intensity-specific comparisons. For the longitudinal effects, functional outcomes were analyzed across timepoints (Pre, Post, Follow-up) as well as single-case comparisons against a control cohort. Neurophysiological outcomes were analyzed within a two-factor design comprising timepoint and stimulation intensity, with analyses focusing on overall timepoint effects and intensity-specific comparisons.

Acknowledgments
We are grateful to Letitia Fisher for her valuable contributions as the clinical coordinator and Nelson Rodriguez for assistance with graphic design. We thank Deena Cilien, DPT and Cristina Segredo, DPT for their expert physical therapy support and for assisting with clinical assessments throughout the study. We also thank Felipe Monteiro, MD and Carlos Blandino for surgical support and Luigi Borda for assistance with the technical design. We extend our sincere gratitude to the research participant for their time, dedication, and insightful contributions throughout the study. This study was supported by The Miami Project to Cure Paralysis, the Buoniconti Foundation, and the Morton Cure Paralysis Fund.

Author contributions
A.S., R.A.F., M.C., and M.M. conceived the research. M.M. and W.D.D. secured the funding. A.S., R.A.F., A.Y., Z.B., H.S., and M.M. designed the experiments, procedures, and assessments. Z.B., K.D., Ni.D., G.S.P., S.T., M.E.I., J.J., A.P., J.D.G., and J.G.C. implemented and evaluated the neurosurgical procedures and participants' clinical management protocols. R.A.F., Z.B., R.deF., Ni.M., E.P., M.C., J.G.C., and M.M. designed and performed the intraoperative monitoring. A.S., R.A.F., A.Y., Z.B., H.S., and Ne.M. performed the experiments. A.S., R.A.F., A.Y., Z.B., H.S., and Ne.M. analyzed the data. A.S. and R.A.F. performed the statistical data analyses. A.S., R.A.F., A.Y., and Z.B. created the figures. Na.D., V.Z., and M.R.P. contributed the control experiment data and performed the procedures. A.S., R.A.F., A.Y., Z.B., H.S., Ne.M., and M.M. wrote the manuscript, and all authors contributed to its editing.

Competing interests
M.E.I. is a consultant to Medtronic, and J.D.G. is a consultant to ONWARD Medical; Neither of these consulting roles are directly related to the work presented in this study. M.R.P. is a co-founder, director, and shareholder in MyndTec Inc., and is also a co-founder and consultant for NovaKonexus. W.D.D. is a co-founder and managing member of InflamaCORE, LLC, and has licensed patents on inflammasome proteins as biomarkers of injury and disease, as well as on targeting inflammasome proteins for therapeutic purposes. W.D.D. is also a Scientific Advisory Board Member of ZyVersa Therapeutics. M.C. holds several patents on spinal cord stimulation for motor recovery and is a shareholder of Reach Neuro Inc., a company developing spinal cord stimulation for post-stroke motor recovery. The remaining authors have no conflicts of interest, financial or otherwise.

Extended Data

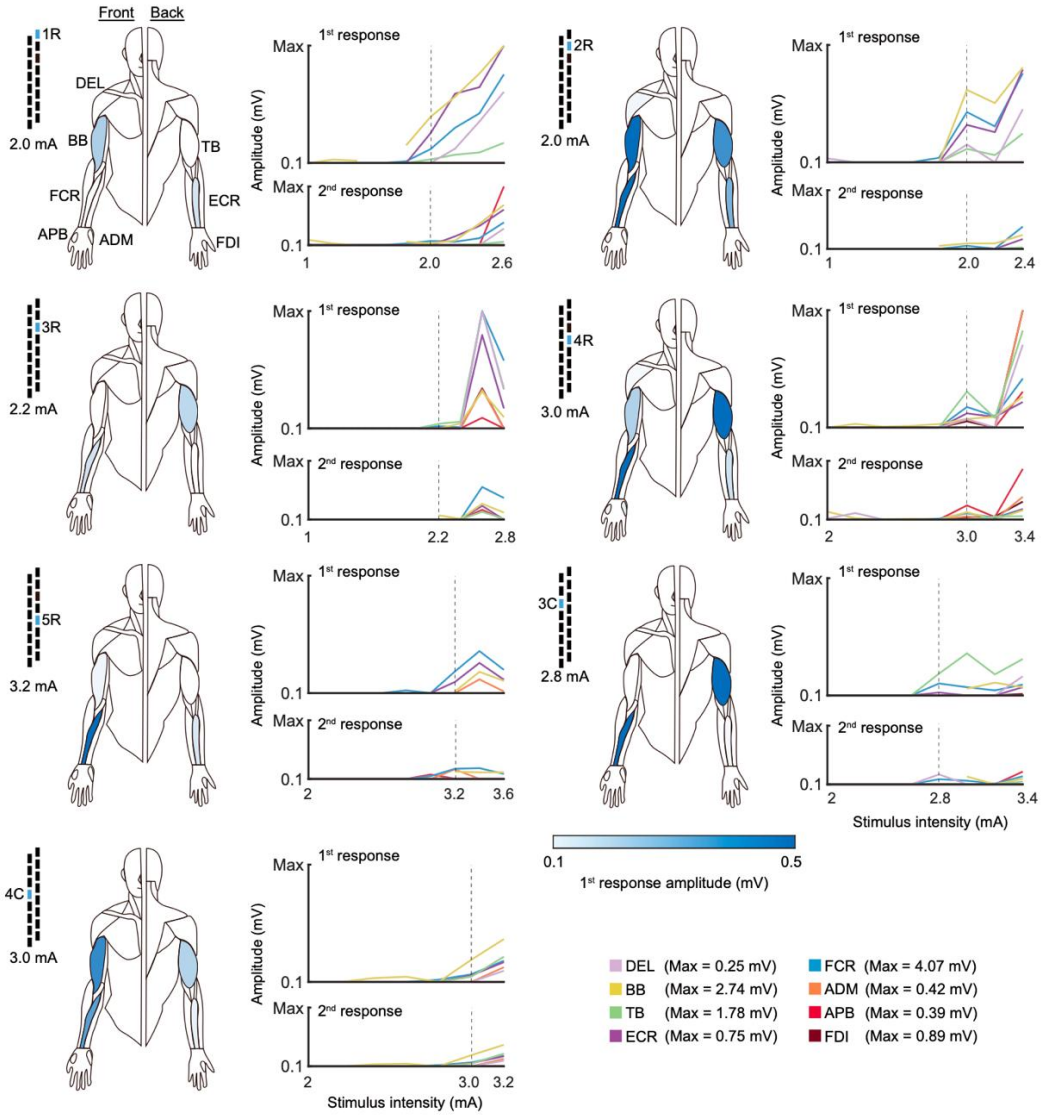

Extended Data Fig. 1: Spinal mapping for optimizing ESCS contacts | Spinal mapping results for optimizing epidural spinal cord stimulation (ESCS) contacts. Stimulation was applied at different contacts along the epidural electrode array, and muscle responses were recorded from multiple upper-limb muscles, including the deltoid (DEL), biceps brachii (BB), triceps brachii (TB), extensor carpi radialis (ECR), flexor carpi radialis (FCR), abductor digiti minimi (ADM), abductor pollicis brevis (APB), and first dorsal interosseous (FDI). Paired-pulse ESCS with incremental stimulation intensities was used to assess the segment-level recruitment curve and to confirm that stimulation predominantly engaged the dorsal roots rather than directly activating motor axons, as indicated by suppression of the second response relative to the first. The left panels illustrate the electrode positions corresponding to each tested contact. The middle panels show human figurines representing predominant muscle activation (first-response amplitude) at stimulation intensities selected on the ascending portion of recruitment curves to demonstrate selective segmental activation. The right panels show recruitment curves of peak-to-peak amplitudes for the first and second responses across increasing stimulation intensities. Y-axes are scaled to each muscle's maximum response across all contacts and intensities. Vertical dotted lines indicate the evoked responses corresponding to the human figurine representations. Truncated portions of the recruitment curve indicate missing data due to spastic responses, particularly in the BB muscle. These spinal mapping results were used to determine the optimal ESCS contacts for neuromodulation and motor engagement during BCI-ESCS therapy.

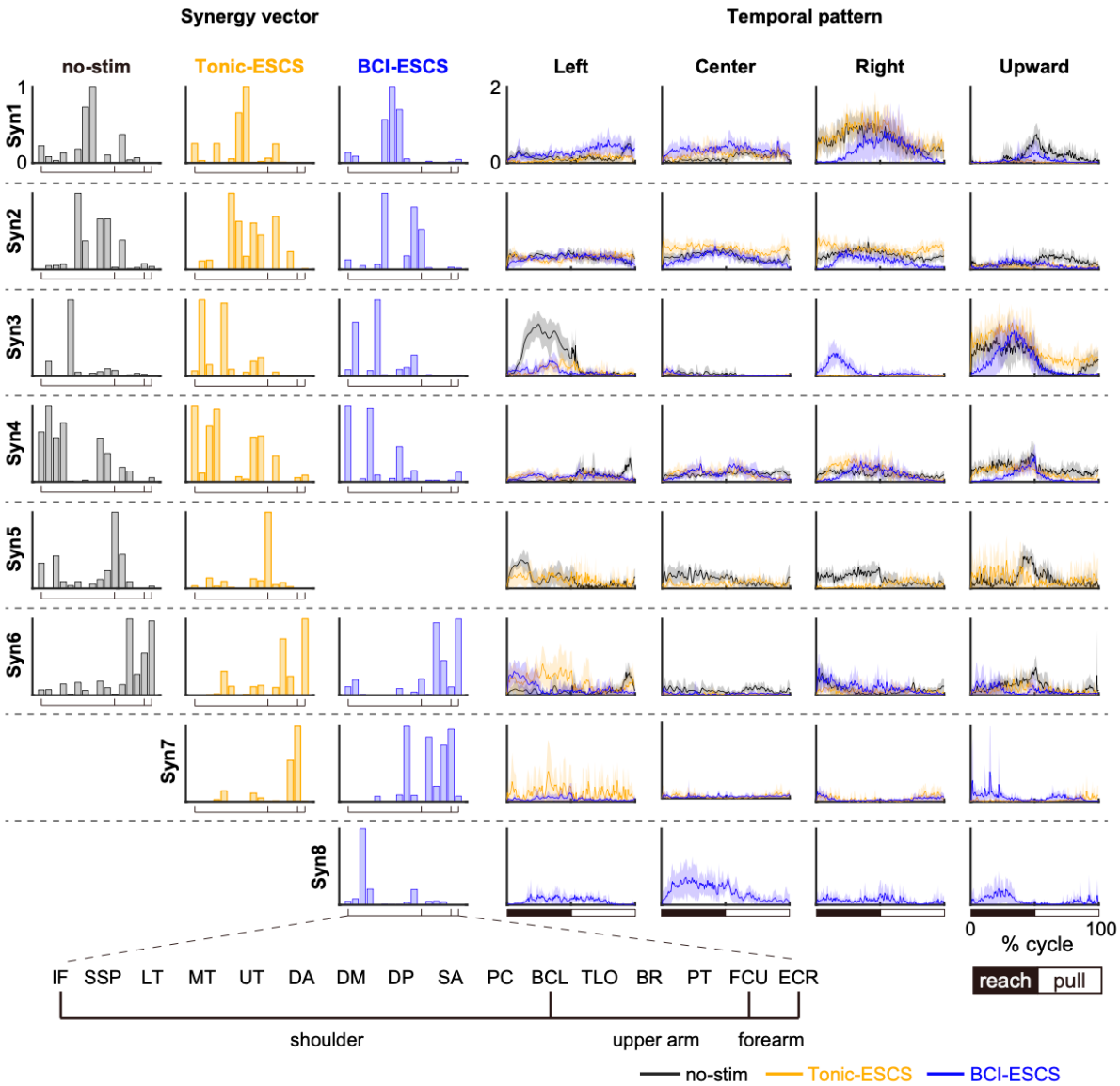

Extended Data Fig. 2: Assistive effects of BCI-ESCS and Tonic-ESCS on muscle synergy | Muscle synergies were extracted under three conditions: no stimulation (no-stim), Tonic-ESCS, and BCI-ESCS. Left panel: Synergy vectors showing muscle contributions. Right panel: Temporal activation patterns during reaching toward left, center, right, and upward targets. Both Tonic-ESCS and BCI-ESCS increased the number of synergies from six (no stimulation) to seven, suggesting a broader movement repertoire with stimulation. Shoulder and wrist-related synergies observed in the no-stimulation condition were fractionated into more functionally distinct synergies under both stimulation conditions, indicating improved coordination. Additionally, BCI-ESCS uniquely facilitated scapular stabilizer activation (LT), suggesting enhanced shoulder control. These findings indicate that stimulation-assisted reaching promotes more adaptive motor control strategies, with BCI-ESCS potentially offering greater benefits for upper limb coordination.
Muscle abbreviations: BCL: biceps (long head), BR: brachioradialis, DA: anterior deltoid, DM: middle deltoid, DP: posterior deltoid, ECR: extensor carpi radialis longus, FCU: flexor carpi ulnaris, IF: infraspinatus, LT: lower trapezius, MT: middle trapezius, PC: pectoralis, PT: pronator teres, SA: serratus anterior, SSP: supraspinatus, TLO: triceps (long head), UT: upper trapezius.

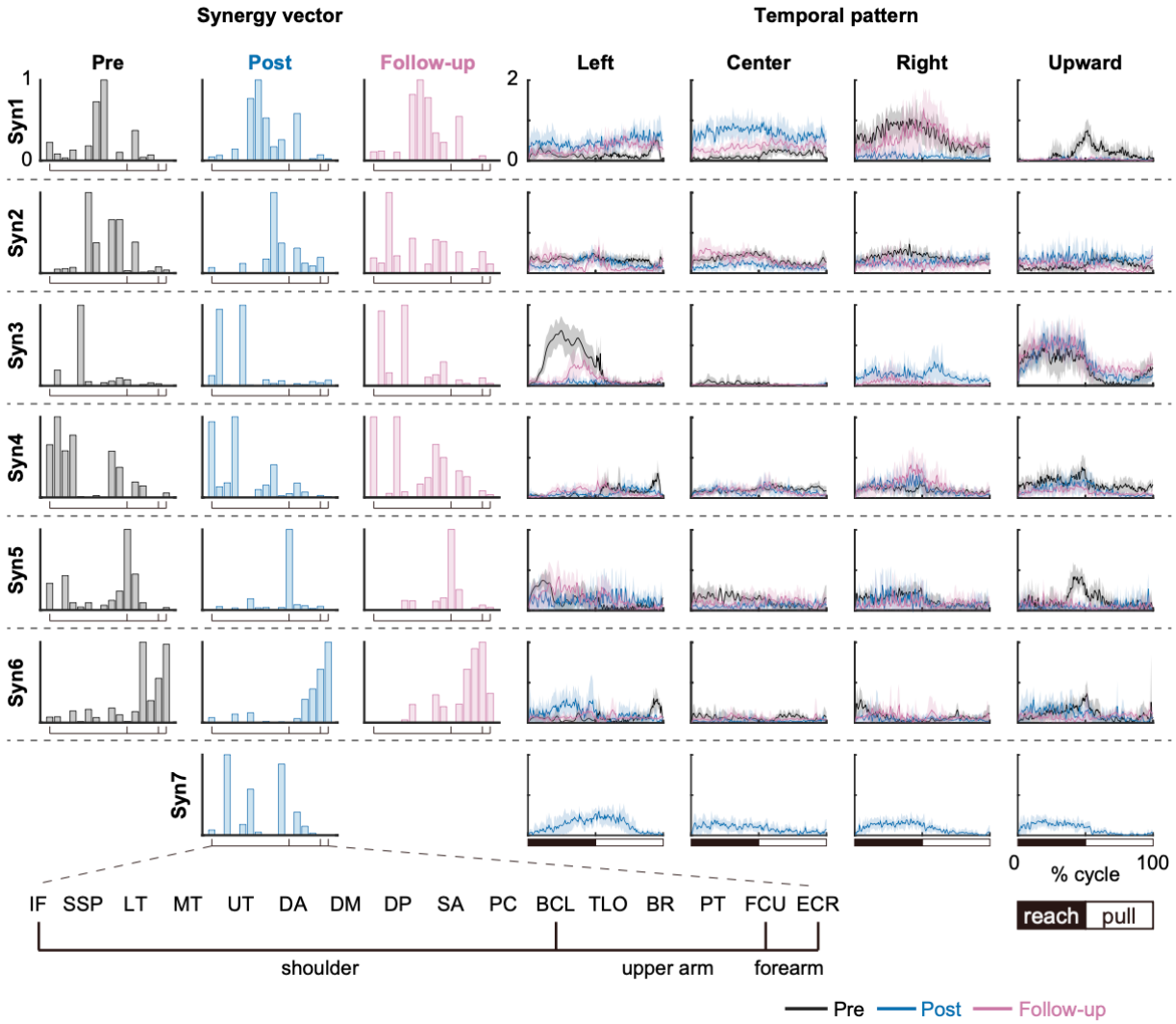

Extended Data Fig. 3: Longitudinal effects of BCI-ESCS therapy on muscle synergy | Muscle synergies were extracted before therapy (Pre), after four weeks of BCI-ESCS therapy (Post), and one month after lead explantation (Follow-up). Left panel: Synergy vectors showing muscle contributions. Right panel: Temporal activation patterns during reaching toward different targets. BCI-ESCS therapy increased the number of muscle synergies (from 6 to 7), reflecting enhanced facilitation of shoulder-related synergies even without stimulation. During the center-target task, improved peak velocity was associated with increased activation of shoulder muscles (DA, DM, DP) in Syn1. Shoulder-related synergies observed pre-therapy (Syn4) were fractionated post-therapy into Syn3 (SSP, UT) and Syn4 (IF, MT), indicating improved scapular-shoulder coordination. Additionally, a novel synergy involving LT, a primary scapular upward rotator, emerged exclusively post-therapy, contributing to smoother and more coordinated reaching movements. However, at the follow-up, the LT synergy was no longer observed, potentially explaining the reversion of some kinematic outcomes toward baseline levels. Muscle abbreviations: BCL: biceps (long head), BR: brachioradialis, DA: anterior deltoid, DM: middle deltoid, DP: posterior deltoid, ECR: extensor carpi radialis longus, FCU: flexor carpi ulnaris, IF: infraspinatus, LT: lower trapezius, MT: middle trapezius, PC: pectoralis, PT: pronator teres, SA: serratus anterior, SSP: supraspinatus, TLO: triceps (long head), UT: upper trapezius.

Extended Data Table 1: Longitudinal effects of BCI-ESCS therapy, Toronto Rehabilitation Institute–Hand Function Test (TRI-HFT). The assessments were conducted at Pre (baseline, before ESCS implantation), Post (after 4 weeks of BCI-ESCS therapy), and Follow-up (4 weeks after ESCS explantation).

Object manipulation		Pre		Post		Follow-up	
		R	L	R	L	R	L
Ten objects							
1. Mug		4	4	4	4	4	4
2. Paper		1	1	2	1	4	1
3. Book		1	1	1	1	1	1
4. Ziplock bag		2	2	2	2	2	2
5. Pop can		1	2	2	2	2	2
6. Dice		4	2	4	2	4	2
7. Sponge		1	1	1	1	1	1
8. Credit card		1	1	4	1	4	4
9. Mobile phone		2	2	6	6	6	4
10. Pencil		2	2	2	2	2	2
Subtotal (70)		19	18	28	22	30	23
Subtotal R+L (140)		37		50		53	
Rectangular blocks							
Weight	Surface friction level						
100 g	high	4	4	4	4	4	4
	middle	1	4	4	4	4	4
	low	2	4	4	4	4	4
200 g	high	2	4	4	4	4	4
	middle	2	4	4	4	4	4
	low	2	2	4	4	4	4
300 g	high	2	2	4	4	4	4
	middle	2	2	4	4	4	4
	low	2	2	4	2	4	2
Subtotal (63)		19	28	36	34	36	34
Subtotal R+L (127)		47		70		70	

Extended Data Table 2: Longitudinal effects of BCI-ESCS therapy, Graded Redefined Assessment of Strength, Sensibility and Prehension (GRASSP). The assessments were conducted at Pre (baseline, before ESCS implantation), Post (after 4 weeks of BCI-ESCS therapy), and Follow-up (4 weeks after ESCS explantation).

	Pre		Post		Follow-up	
	R	L	R	L	R	L
Strength	7	10	8	9	8	9
Sensory- Dorsal	0	0	0	3	0	1
Sensory- Palmar	1	4	2	0	0	0
Prehension-Qualitative	2	2	2	1	2	1
Prehension-Quantitative	2	6	6	5	5	5
Total	12	22	18	18	15	16

References

1. Anderson, K. D. Targeting Recovery: Priorities of the Spinal Cord-Injured Population. *Journal of Neurotrauma* **21**, 1371–1383 (2004).
2. Thompson, C., Mutch, J., Parent, S. & Mac-Thiong, J.-M. The changing demographics of traumatic spinal cord injury: An 11-year study of 831 patients. *The Journal of Spinal Cord Medicine* **38**, 214–223 (2015).
3. Tanadini, L. G. *et al.* Identifying Homogeneous Subgroups in Neurological Disorders: Unbiased Recursive Partitioning in Cervical Complete Spinal Cord Injury. *Neurorehabil Neural Repair* **28**, 507–515 (2014).
4. Kirshblum, S. & Waring, W. Updates for the International Standards for Neurological Classification of Spinal Cord Injury. *Physical Medicine and Rehabilitation Clinics of North America* **25**, 505–517 (2014).
5. Harkema, S. *et al.* Effect of epidural stimulation of the lumbosacral spinal cord on voluntary movement, standing, and assisted stepping after motor complete paraplegia: a case study. *The Lancet* **377**, 1938–1947 (2011).
6. Angeli, C. A., Edgerton, V. R., Gerasimenko, Y. P. & Harkema, S. J. Altering spinal cord excitability enables voluntary movements after chronic complete paralysis in humans. *Brain* **137**, 1394–1409 (2014).
7. Wagner, F. B. *et al.* Targeted neurotechnology restores walking in humans with spinal cord injury. *Nature* **563**, 65–71 (2018).
8. Gill, M. L. *et al.* Neuromodulation of lumbosacral spinal networks enables independent stepping after complete paraplegia. *Nat Med* **24**, 1677–1682 (2018).

9. Romeni, S. *et al.* High-frequency epidural electrical stimulation reduces spasticity and facilitates walking recovery in patients with spinal cord injury. *Sci. Transl. Med.* **17**, eadp9607 (2025).
10. Greiner, N. *et al.* Recruitment of upper-limb motoneurons with epidural electrical stimulation of the cervical spinal cord. *Nat Commun* **12**, 435 (2021).
11. Barra, B. *et al.* Epidural electrical stimulation of the cervical dorsal roots restores voluntary upper limb control in paralyzed monkeys. *Nature Neuroscience* **25**, 924–934 (2022).
12. Lu, D. C. *et al.* Engaging Cervical Spinal Cord Networks to Reenable Volitional Control of Hand Function in Tetraplegic Patients. *Neurorehabil Neural Repair* **30**, 951–962 (2016).
13. Powell, M. P. *et al.* Epidural stimulation of the cervical spinal cord for post-stroke upper-limb paresis. *Nat Med* **29**, 689–699 (2023).
14. Ajiboye, A. B. *et al.* Restoration of reaching and grasping movements through brain-controlled muscle stimulation in a person with tetraplegia: a proof-of-concept demonstration. *The Lancet* **389**, 1821–1830 (2017).
15. Bouton, C. E. *et al.* Restoring cortical control of functional movement in a human with quadriplegia. *Nature* **533**, 247–250 (2016).
16. Ethier, C., Oby, E. R., Bauman, M. J. & Miller, L. E. Restoration of grasp following paralysis through brain-controlled stimulation of muscles. *Nature* **485**, 368–371 (2012).
17. Capogrosso, M. *et al.* A brain–spine interface alleviating gait deficits after spinal cord injury in primates. *Nature* **539**, 284–288 (2016).
18. Lorach, H. *et al.* Walking naturally after spinal cord injury using a brain–spine interface. *Nature* **618**, 126–133 (2023).

19. Samejima, S. *et al.* Brain-Computer-Spinal Interface Restores Upper Limb Function After Spinal Cord Injury. *IEEE Trans. Neural Syst. Rehabil. Eng.* **29**, 1233–1242 (2021).
20. Kato, K., Sawada, M. & Nishimura, Y. Bypassing stroke-damaged neural pathways via a neural interface induces targeted cortical adaptation. *Nat Commun* **10**, 4699 (2019).
21. Schirmer, C. M. *et al.* Heuristic map of myotomal innervation in humans using direct intraoperative nerve root stimulation: Clinical article. *Journal of Neurosurgery: Spine* **15**, 64–70 (2011).
22. Cajigas, I. *et al.* Implantable brain–computer interface for neuroprosthetic-enabled volitional hand grasp restoration in spinal cord injury. *Brain Communications* **3**, fcab248 (2021).
23. Davis, K. C. *et al.* 5-year follow-up of a fully implanted brain–computer interface in a spinal cord injury patient. *J. Neural Eng.* **22**, 026050 (2025).
24. Márquez-Chin, C., Popovic ,Milos R., Sanin ,Egor, Chen ,Robert & and Lozano, A. M. Real-time two-dimensional asynchronous control of a computer cursor with a single subdural electrode. *The Journal of Spinal Cord Medicine* **35**, 382–391 (2012).
25. Jovanovic, L. I. *et al.* Brain–computer interface-triggered functional electrical stimulation therapy for rehabilitation of reaching and grasping after spinal cord injury: a feasibility study. *Spinal Cord Series and Cases* **7**, 24 (2021).
26. Jovanovic, L. I., Popovic ,Milos R. & and Marquez-Chin, C. KITE-BCI: A brain-computer interface system for functional electrical stimulation therapy. *The Journal of Spinal Cord Medicine* **44**, S203–S214 (2021).
27. Fadli, R. A. *et al.* Effectiveness of motor and prefrontal cortical areas for brain-controlled functional electrical stimulation neuromodulation. *Journal of Neural Engineering* **20**, 056022 (2023).

28. Suzuki, Y. *et al.* Evidence That Brain-Controlled Functional Electrical Stimulation Could Elicit Targeted Corticospinal Facilitation of Hand Muscles in Healthy Young Adults. *Neuromodulation* **26**, 1612–1621 (2023).
29. Shingane, S. N., Rao, N., Kumar, N. & Mutha, P. K. Task relevance selectively modulates sensorimotor adaptation in the presence of multiple prediction errors. *Journal of Neurophysiology* **134**, 1607–1618 (2025).
30. Coderre, A. M. *et al.* Assessment of Upper-Limb Sensorimotor Function of Subacute Stroke Patients Using Visually Guided Reaching. *Neurorehabil Neural Repair* **24**, 528–541 (2010).
31. Hayes, H. B., Chvatal, S. A., French, M. A., Ting, L. H. & Trumbower, R. D. Neuromuscular constraints on muscle coordination during overground walking in persons with chronic incomplete spinal cord injury. *Clinical Neurophysiology* **125**, 2024–2035 (2014).
32. Cheung, V. C. K. *et al.* Muscle synergy patterns as physiological markers of motor cortical damage. *Proceedings of the National Academy of Sciences* **109**, 14652–14656 (2012).
33. Anderson, K. D. *et al.* Multi-center, single-blind randomized controlled trial comparing functional electrical stimulation therapy to conventional therapy in incomplete tetraplegia. *Front. Rehabilit. Sci.* **3**, 995244 (2022).
34. Kalsi-Ryan, S. *et al.* Responsiveness, Sensitivity, and Minimally Detectable Difference of the Graded and Redefined Assessment of Strength, Sensibility, and Prehension, Version 1.0. *Journal of Neurotrauma* **33**, 307–314 (2016).
35. Oudega, M. & Perez, M. A. Corticospinal reorganization after spinal cord injury: Corticospinal tract and SCI. *The Journal of Physiology* **590**, 3647–3663 (2012).

36. de Freitas, R. M. *et al.* SPINAL CORD STIMULATION IMPROVES MOTOR FUNCTION AND SPASTICITY IN CHRONIC POST-STROKE UPPER LIMB HEMIPARESIS. *medRxiv* 2025.08.01.25332445 (2025) doi:10.1101/2025.08.01.25332445.
37. Capogrosso, M. *et al.* A Computational Model for Epidural Electrical Stimulation of Spinal Sensorimotor Circuits. *Journal of Neuroscience* **33**, 19326–19340 (2013).
38. Rattay, F., Minassian, K. & Dimitrijevic, M. Epidural electrical stimulation of posterior structures of the human lumbosacral cord: 2. quantitative analysis by computer modeling. *Spinal Cord* **38**, 473–489 (2000).
39. Guiho, T., Baker, S. N. & Jackson, A. Epidural and transcutaneous spinal cord stimulation facilitates descending inputs to upper-limb motoneurons in monkeys. *J. Neural Eng.* **18**, 046011 (2021).
40. Balaguer, J.-M. *et al.* Supraspinal control of motoneurons after paralysis enabled by spinal cord stimulation.
41. Nishimura, Y., Perlmutter, S. I. & Fetz, E. E. Restoration of upper limb movement via artificial corticospinal and musculospinal connections in a monkey with spinal cord injury. *Front. Neural Circuits* **7**, (2013).
42. Biasiucci, A. *et al.* Brain-actuated functional electrical stimulation elicits lasting arm motor recovery after stroke. *Nat Commun* **9**, 2421 (2018).
43. Balbinot, G. *et al.* Segmental motor recovery after cervical spinal cord injury relates to density and integrity of corticospinal tract projections. *Nat Commun* **14**, 723 (2023).
44. Jo, H. J. & Perez, M. A. Corticospinal-motor neuronal plasticity promotes exercise-mediated recovery in humans with spinal cord injury. *Brain* **143**, 1368–1382 (2020).

45. Sangari, S. & Perez, M. A. Distinct Corticospinal and Reticulospinal Contributions to Voluntary Control of Elbow Flexor and Extensor Muscles in Humans with Tetraplegia. *J. Neurosci.* **40**, 8831–8841 (2020).

46. Bunday, K. L. & Perez, M. A. Motor Recovery after Spinal Cord Injury Enhanced by Strengthening Corticospinal Synaptic Transmission. *Current Biology* **22**, 2355–2361 (2012).

47. Osuagwu, B. C. A., Wallace, L., Fraser, M. & Vuckovic, A. Rehabilitation of hand in subacute tetraplegic patients based on brain computer interface and functional electrical stimulation: a randomised pilot study. *Journal of Neural Engineering* **13**, 065002 (2016).

48. Jackson, A. & Zimmermann, J. B. Neural interfaces for the brain and spinal cord—restoring motor function. *Nat Rev Neurol* **8**, 690–699 (2012).

49. Bonizzato, M. *et al.* Brain-controlled modulation of spinal circuits improves recovery from spinal cord injury. *Nat Commun* **9**, 3015 (2018).

50. Markram, H. A history of spike-timing-dependent plasticity. *Front. Syn. Neurosci.* **3**, (2011).

51. Zheng, B. & Tuszynski, M. H. Regulation of axonal regeneration after mammalian spinal cord injury. *Nat Rev Mol Cell Biol* **24**, 396–413 (2023).

52. Courtine, G. *et al.* Recovery of supraspinal control of stepping via indirect propriospinal relay connections after spinal cord injury. *Nature Medicine* **14**, 69–74 (2008).

53. Gad, P. *et al.* Non-Invasive Activation of Cervical Spinal Networks after Severe Paralysis. *Journal of Neurotrauma* **35**, 2145–2158 (2018).

54. Inanici, F., Brighton, L. N., Samejima, S., Hofstetter, C. P. & Moritz, C. T. Transcutaneous Spinal Cord Stimulation Restores Hand and Arm Function After Spinal Cord Injury. *IEEE Trans. Neural Syst. Rehabil. Eng.* **29**, 310–319 (2021).

55. Moritz, C. *et al.* Non-invasive spinal cord electrical stimulation for arm and hand function in chronic tetraplegia: a safety and efficacy trial. *Nat Med* **30**, 1276–1283 (2024).

56. Chen, B. *et al.* Combinatorial approaches increasing neuronal activity accelerate recovery after spinal cord injury. *Brain* **148**, 1911–1923 (2025).

57. Ribeiro, B. F. *et al.* Cell therapies for spinal cord injury: a review of the clinical trials and cell-type therapeutic potential. *Brain* **146**, 2672–2693 (2023).

58. Finney, J. N. *et al.* Techniques to mitigate lead migration for percutaneous trials of cervical spinal cord stimulation. *Frontiers in Surgery* **Volume 12-2025**, (2025).

59. Milosevic, M., Masugi, Y., Sasaki, A., Sayenko, D. G. & Nakazawa, K. On the reflex mechanisms of cervical transcutaneous spinal cord stimulation in human subjects. *Journal of Neurophysiology* **121**, 1672–1679 (2019).

60. de Freitas, R. M. *et al.* Selectivity and excitability of upper-limb muscle activation during cervical transcutaneous spinal cord stimulation in humans. *Journal of Applied Physiology* **131**, 746–759 (2021).

61. Cajigas, I. *et al.* Brain-Computer interface control of stepping from invasive electrocorticography upper-limb motor imagery in a patient with quadriplegia. *Front. Hum. Neurosci.* **16**, 1077416 (2023).

62. Kapadia, N., Zivanovic, V., Verrier, M. & Popovic, M. Toronto Rehabilitation Institute–Hand Function Test: Assessment of Gross Motor Function in Individuals With Spinal Cord Injury. *Topics in Spinal Cord Injury Rehabilitation* **18**, 167–186 (2012).

63. Kapadia, N. *et al.* Preliminary evaluation of the reliability and validity of the 3D printed Toronto Rehabilitation Institute-Hand Function Test in individuals with spinal cord injury. *The Journal of Spinal Cord Medicine* **44**, S225–S233 (2021).

64. Kapadia, N., Zivanovic, V. & Popovic, M. Restoring Voluntary Grasping Function in Individuals with Incomplete Chronic Spinal Cord Injury: Pilot Study. *Topics in Spinal Cord Injury Rehabilitation* **19**, 279–287 (2013).

65. Kalsi-Ryan, S. *et al.* The Graded Redefined Assessment of Strength Sensibility and Prehension: Reliability and Validity. *Journal of Neurotrauma* **29**, 905–914 (2012).

66. Kalsi-Ryan, S., Curt, A., Fehlings, M. & Verrier, M. Assessment of the Hand in Tetraplegia Using the Graded Redefined Assessment of Strength, Sensibility and Prehension (GRASSP): Impairment Versus Function. *Topics in Spinal Cord Injury Rehabilitation* **14**, 34–46 (2009).

67. Kirshblum, S. C. *et al.* International standards for neurological classification of spinal cord injury (Revised 2011). *The Journal of Spinal Cord Medicine* **34**, 535–546 (2011).

68. Leclere, N. X., Sarlegna, F. R., Coello, Y. & Bourdin, C. Gradual exposure to Coriolis force induces sensorimotor adaptation with no change in peripersonal space. *Scientific Reports* **12**, 922 (2022).

69. Widerström-Noga, E. *et al.* The International Spinal Cord Injury Pain Basic Data Set (version 2.0). *Spinal Cord* **52**, 282–286 (2014).

70. Charlifue, S. *et al.* International Spinal Cord Injury Quality of Life Basic Data Set. *Spinal Cord* **50**, 672–675 (2012).

71. Post, M. W. M. *et al.* Rasch Analysis of the International Quality of Life Basic Data Set Version 2.0. *Archives of Physical Medicine and Rehabilitation* **103**, 2120–2130 (2022).

72. Catz, A. *et al.* A multicenter international study on the Spinal Cord Independence Measure, version III: Rasch psychometric validation. *Spinal Cord* **45**, 275–291 (2007).

73. Bluvshtein, V. *et al.* SCIM III is reliable and valid in a separate analysis for traumatic spinal cord lesions. *Spinal Cord* **49**, 292–296 (2011).

74. Earhart, G. M. *et al.* The 9-Hole Peg Test of Upper Extremity Function: Average Values, Test-Retest Reliability, and Factors Contributing to Performance in People With Parkinson Disease. *Journal of Neurologic Physical Therapy* **35**, (2011).

75. Feys, P. *et al.* The Nine-Hole Peg Test as a manual dexterity performance measure for multiple sclerosis. *Mult Scler* **23**, 711–720 (2017).

76. Mathiowetz, V., Federman, S. & Wiemer, D. Box and Block Test of Manual Dexterity: Norms for 6–19 Year Olds. *Can J Occup Ther* **52**, 241–245 (1985).

77. Oliveira, C. S. *et al.* Use of the Box and Block Test for the evaluation of manual dexterity in individuals with central nervous system disorders: A systematic review. *mtprehabjournal* 1–7 (2016).

78. Akpinar, P. *et al.* Reliability of the Modified Ashworth Scale and Modified Tardieu Scale in patients with spinal cord injuries. *Spinal Cord* **55**, 944–949 (2017).